



Support:



# Nanoplasmonics: Optical Properties of Plasmonic Nanosystems

## Mark I. Stockman

Department of Physics and Astronomy, Georgia State  
University, Atlanta, GA 30303, USA

Lecture 2:

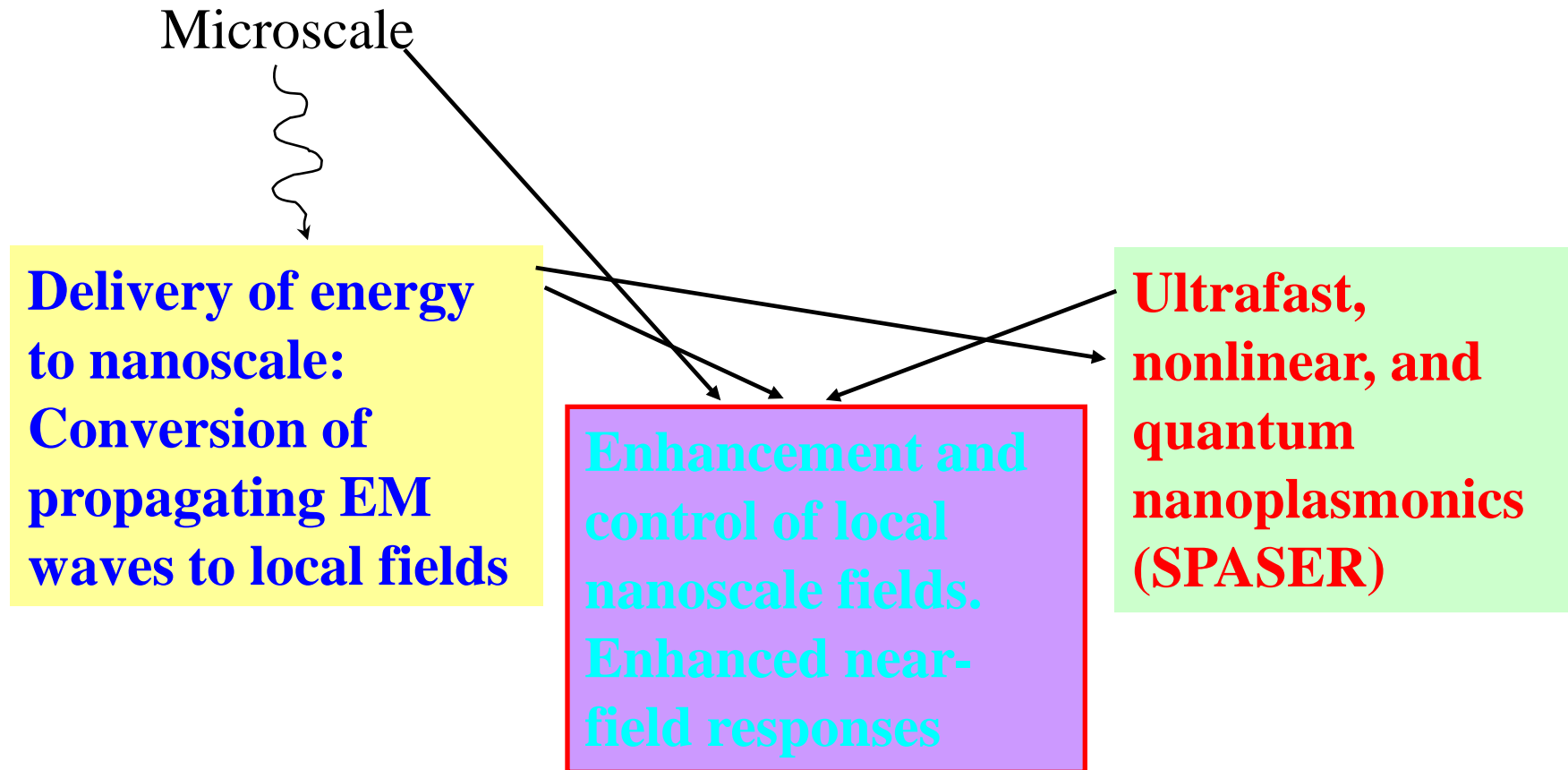
# Nanoplasmonics of Nanosystems

## LECTURE 2

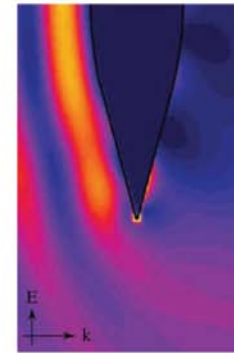
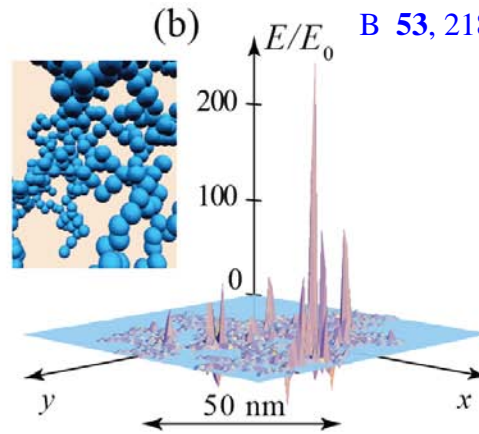
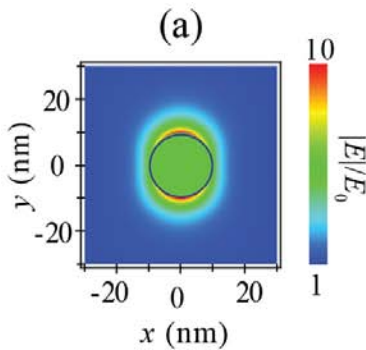
# Nanoplasmonics of Nanosystems

1. Introduction; Local fields of a sphere and lifetimes
2. Localized SP resonances (SPs or LSPRs): Quasistatic eigenmodes
3. Nanoshells, their eigenmodes and absorption cross section
4. SERS
5. Applications to nanoscopy
6. Aggregates of nanospheres; nanolenses
7. Extreme nanoplasmonics (optional)

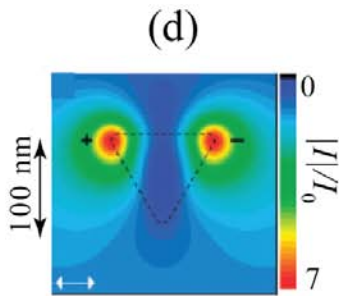
## PROBLEMS IN NANOOPTICS



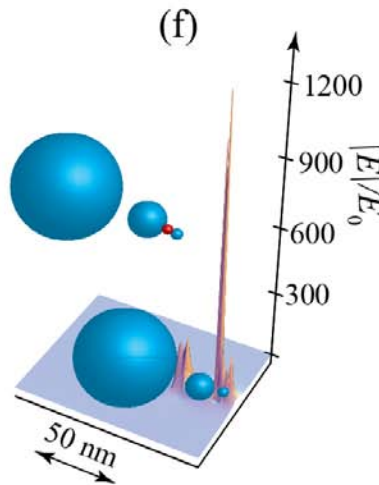
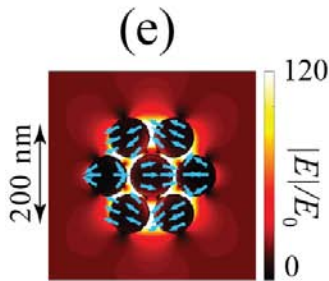
- M. I. Stockman et al., *Phys. Rev. Lett.* **75**, 2450 (1995)
- M. I. Stockman, L. N. Pandey, and T. F. George, *Phys. Rev. B* **53**, 2183-2186 (1996)



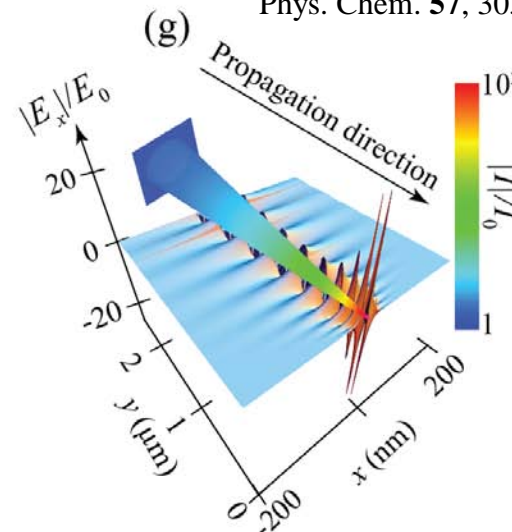
L. Novotny and S. J. Stranick, *Annual Rev. Phys. Chem.* **57**, 303-331 (2006)



M. Rang et al., *Nano Lett.* **8**, 3357 (2008)



K. Li, M. I. Stockman, and D. J. Bergman, *Phys. Rev. Lett.* **91**, 227402 (2003)



M. I. Stockman, *Phys. Rev. Lett.* **93**, 137404 (2004)

- J. A. Fan et al., *Science* **328**, 1135 (2010)
- M. Hentschel et al., *Nano Lett.* **10**, 2721 (2010)

# Quasistatic Approximation and Eigenmodes

For a nanosystem, size is much less than the radiation wavelength and skin depth. In this case, one can neglect retardation, and describe the system by quasistatic equations for electrostatic potential.

Quasistatic approximation does not imply that the excitation processes are slow. Just to the opposite, the neglectable retardation allows one to use and study ultrafast processes in nanostructures.

## Quasistatic Field Equations and Boundary Conditions

$$\frac{\partial}{\partial \mathbf{r}} \varepsilon(\mathbf{r}, \omega) \frac{\partial}{\partial \mathbf{r}} \varphi(\mathbf{r}) = 0, \quad \varphi(x, y, 0) = 0, \quad \varphi(x, y, L_z) = 1,$$

$$\left. \frac{\partial}{\partial x} \varphi(x, y, z) \right|_{x=0, L_x} = \left. \frac{\partial}{\partial y} \varphi(x, y, z) \right|_{y=0, L_y} = 0.$$

# Quasistatic Fields as Expansion over Eigenmodes for Spherical Particles

$$\varphi_2(l, m, r, \theta, \varphi) = \left[ a_2(l, m) \frac{1}{r^{l+1}} + b_2(l, m) r^l \right] Y_{lm}(\theta, \varphi),$$

$$\varphi_1(l, m, r, \theta, \varphi) = \left[ a_1(l, m) \frac{1}{r^{l+1}} + b_1(l, m) r^l \right] Y_{lm}(\theta, \varphi).$$

Consider 1 as internal region and 2 as external.

Unity field at the infinity is given by a choice  $b_2(l, m) = -1$ ;

Regularity in the center requires  $a_1(l, m) = 0$ .

Maxwell boundary conditions at the surface of the sphere:

$$\varphi_1(l, m, R, \theta, \phi) = \varphi_2(l, m, R, \theta, \phi);$$

$$\varepsilon_1 \frac{\partial}{\partial R} \varphi_1(l, m, R, \theta, \phi) = \varepsilon_2 \frac{\partial}{\partial R} \varphi_2(l, m, R, \theta, \phi).$$

Coefficients of eigenmodes expansion for  $L$ -multipole mode:

$$a_2(l, m) = \frac{R^{2l+1}l(\varepsilon_1 - \varepsilon_2)}{\varepsilon_2 + l(\varepsilon_1 + \varepsilon_2)}; \quad b_1(l, m) = \frac{(1+2l)\varepsilon_2}{\varepsilon_2 + l(\varepsilon_1 + \varepsilon_2)}; \quad .$$

$$l - \text{multipolar polarizability: } \alpha_l = R^{2l+1} \frac{l(\varepsilon_1 - \varepsilon_2)}{\varepsilon_2 + l(\varepsilon_1 + \varepsilon_2)};$$

$$\text{Dipolar polarizability: } \alpha_1 = a_2(1, m) = R^3 \frac{\varepsilon_1 - \varepsilon_2}{\varepsilon_1 + 2\varepsilon_2};$$

$$\text{In usual notations (1} \rightarrow \text{m, 2} \rightarrow \text{d): } \alpha = R^3 \frac{\varepsilon_m - \varepsilon_d}{\varepsilon_m + 2\varepsilon_d}.$$

$$\text{Surface plasmon resonance of a sphere: } \text{Re} \varepsilon_m(\omega_{sp}) = -2\varepsilon_d .$$



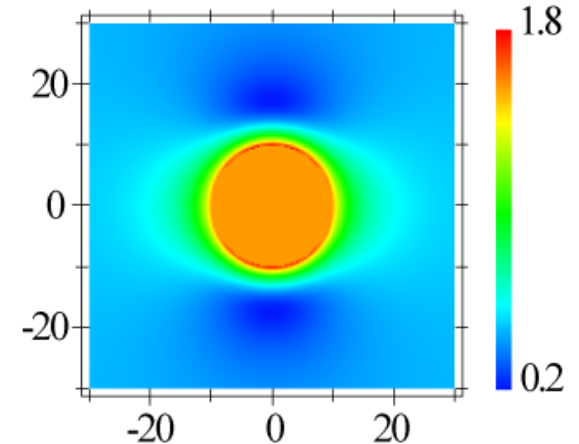
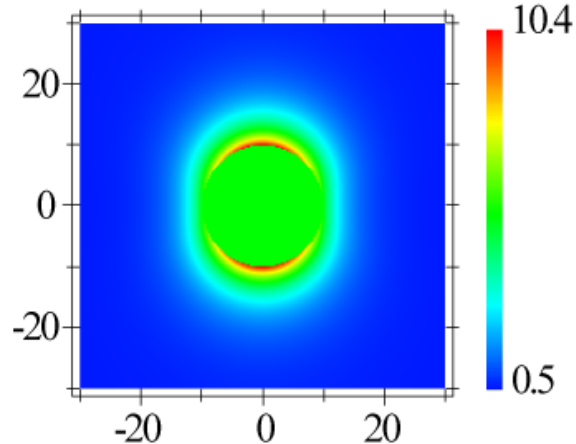
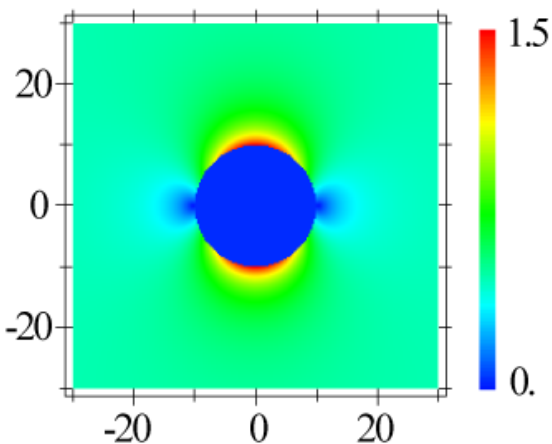
# Quasistatic Local Field Magnitude for Silver Nanosphere in Vacuum

Excitation Polarization

$\hbar\omega = 1.55 \text{ eV} < \hbar\omega_{SP}$

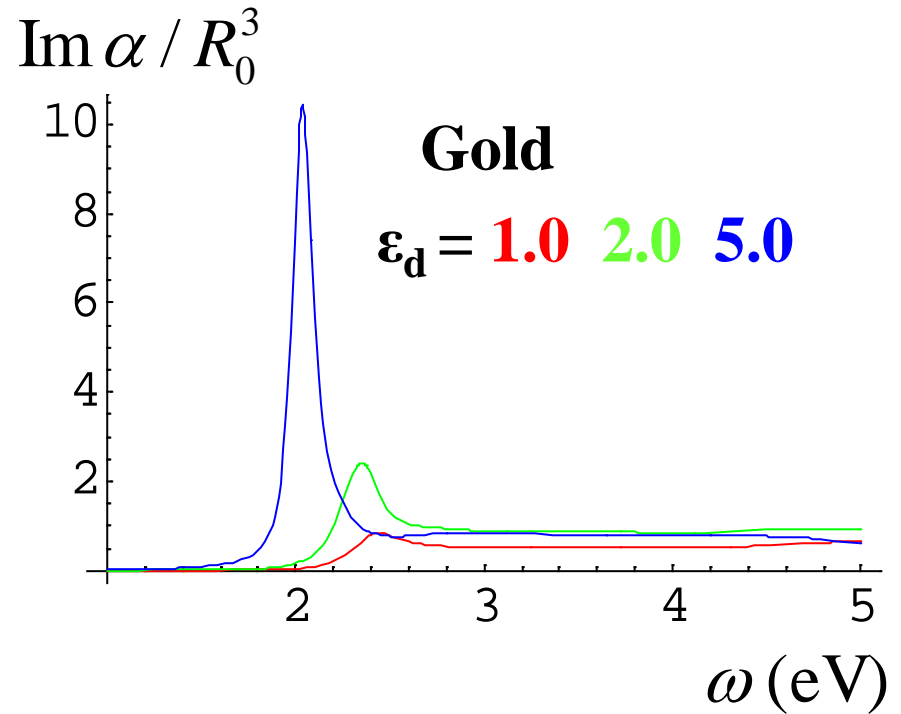
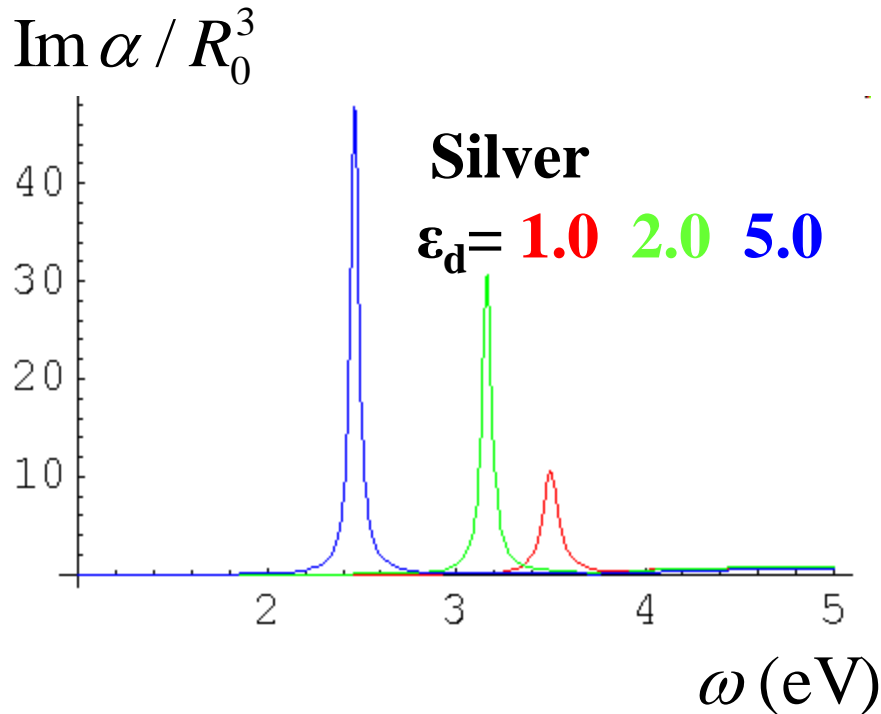
$\hbar\omega = 3.51 \text{ eV} = \hbar\omega_{SP}$

$\hbar\omega = 3.65 \text{ eV} > \hbar\omega_{SP}$



## Total extinction (absorption + scattering) cross section

(Optical Theorem) 
$$\sigma_{tot} = 2\pi \frac{\omega}{c} \text{Im } \alpha, \quad \alpha = R_0^3 \frac{\epsilon_m - \epsilon_d}{\epsilon_m + 2\epsilon_d}$$



# Quantum plasmon resonances of individual metallic nanoparticles

Jonathan A. Scholl<sup>1</sup>, Ai Leen Koh<sup>2</sup> & Jennifer A. Dionne<sup>1</sup>

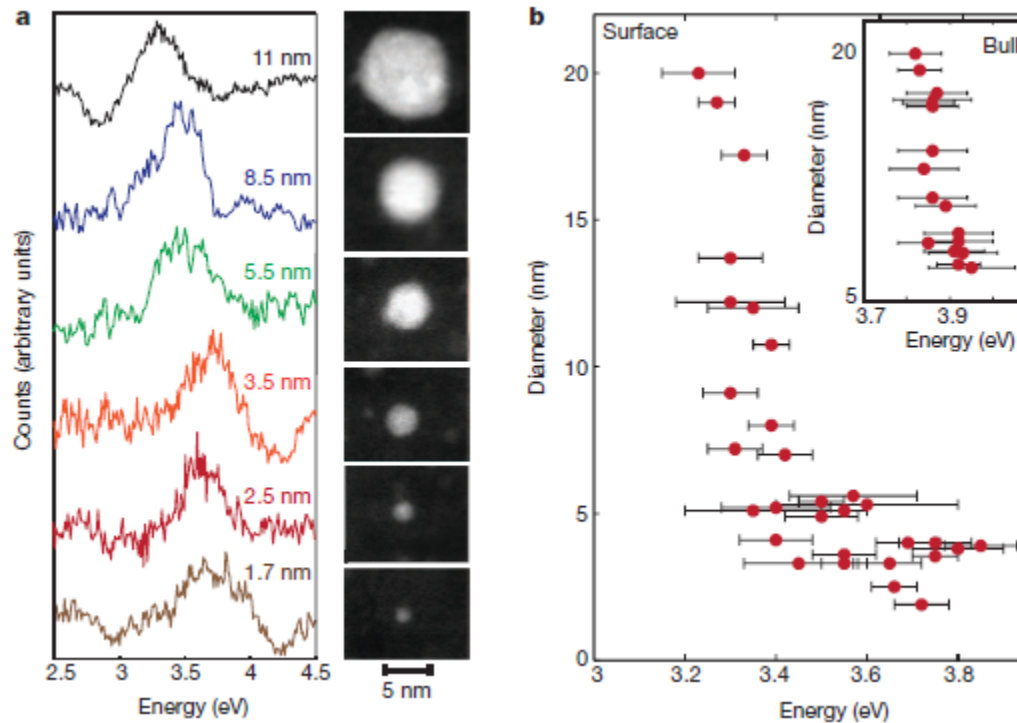


**Figure 3 | Correlating Ag nanoparticle geometry with plasmonic EELS data.** **a**, Collection of normalized, deconvoluted EELS data from particles ranging from 11 nm to 1.7 nm in diameter and the corresponding STEM image of each specimen. The electron beam was directed onto the edge of the particles so that only the surface resonance is shown. **b**, Plot of the surface plasmon resonance

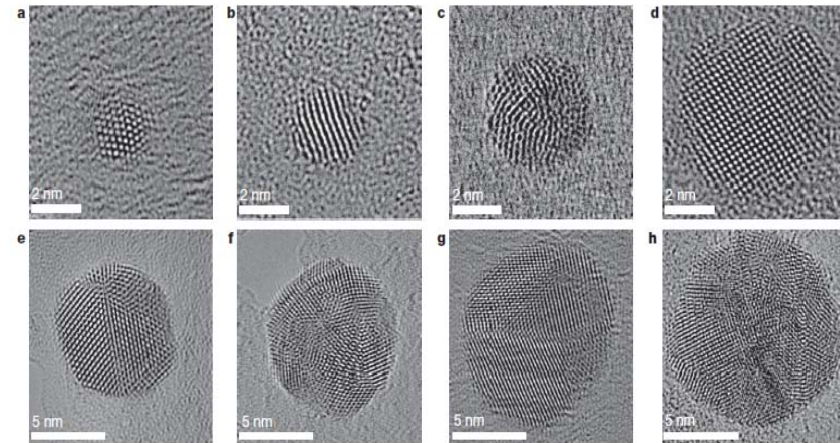


**Figure 1 |** Aberration-corrected TEM images of silver nanoparticles synthesized free of stabilizing ligands. Particles with diameters of 2 nm (**a**), 3 nm (**b**), 4.5 nm (**c**), 6 nm (**d**), 7.5 nm (**e**), 9 nm (**f**), 10.5 nm (**g**), and 12 nm (**h**) are shown. Scale bars: **a**–**d**, 2 nm; **e**–**h**, 5 nm.

energy versus particle diameter, with the inset depicting bulk resonance energies. Horizontal error bars indicating 95% confidence intervals were generated with a curve fitting and bootstrapping technique (see Methods). Vertical error bars are contained within the size of the data points.

# Plasmon Lifetimes

General behavior of polarizability close to a (plasmon) pole  
[See: V. B. Berestetskii, E. M. Lifshits, and L. P. Pitaevskii, *Quantum Electrodynamics* (Pergamon Press, Oxford and New York, 1982)]:

$$\alpha = \frac{|\mathbf{d}_{0p}|^2}{\hbar(\omega - \omega_p)}$$

Compare this to the polarizability of a nanosphere:

$$\alpha = R^3 \frac{\varepsilon_m(\omega) - \varepsilon_d}{\varepsilon_m(\omega) + 2\varepsilon_d} \approx R^3 \frac{-3\varepsilon_d}{(\omega - \omega_p) \left. \frac{\partial(\text{Re } \varepsilon_m(\omega))}{\partial \omega} \right|_{\omega = \omega_p}},$$

where  $\text{Re } \varepsilon_m(\omega_p) = -2\varepsilon_d$

From this, we find the transition dipole of a plasmon:

$$|\mathbf{d}_{0p}|^2 = \hbar R^3 \frac{3\varepsilon_d}{\left. \frac{\partial(\text{Re } \varepsilon_m(\omega))}{\partial\omega} \right|_{\omega = \omega_p}}$$

Substituting it into standard formula for radiative decay rate,

$$\gamma_n^{(r)} = \frac{4}{3} \frac{\omega_n^3 \sqrt{\varepsilon_d}}{\hbar c^3} |(\mathbf{d})_{n0}|^2, \text{ we obtain:}$$

$$\gamma_r = 4 \left( \frac{\omega R}{c} \right)^3 \frac{\varepsilon_d}{\left. \frac{\partial(\text{Re } \varepsilon_m(\omega))}{\partial\omega} \right|_{\omega = \omega_p}}$$

**Nonradiative decay rate** can be found from the pole of the polarizability

$$\varepsilon_m(\omega_p - i\gamma_{nr}) + 2\varepsilon_d = 0$$

Expanding, we find the non-radiative rate

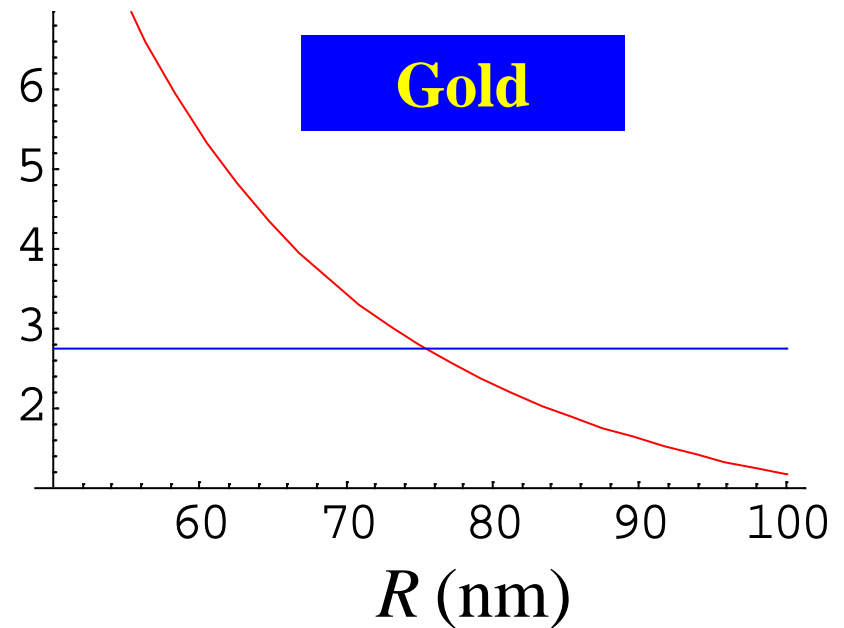
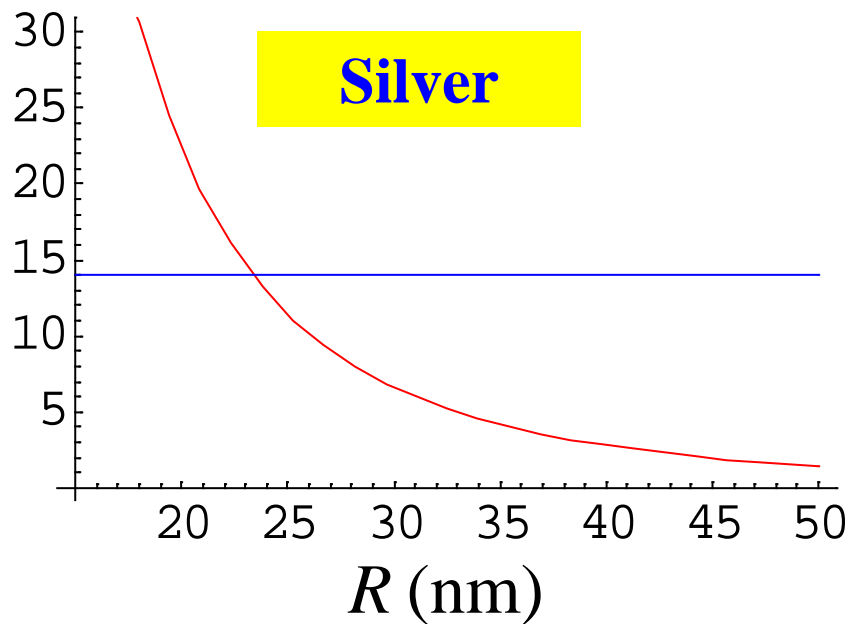
$$\gamma_{nr} = \frac{\text{Im } \varepsilon_m(\omega_p)}{\left. \frac{\partial(\text{Re } \varepsilon_m(\omega))}{\partial \omega} \right|_{\omega = \omega_p}}$$

Comparing to the radiative rate:

$$\frac{\gamma_r}{\gamma_{nr}} = 4 \left( \frac{R}{\tilde{\lambda}} \right)^3 \frac{1}{\text{Im } \varepsilon_m(\omega_p)}$$

Nonradiative lifetime (fs):  $\tau_{nr} = \frac{1}{\gamma_{nr}}$

Radiative lifetime (fs):  $\tau_r = \frac{1}{\gamma_r}$



**We will follow the spectral theory** that allows one to *separate the material and geometric properties of the system.*

1. D. J. Bergman and D. Stroud, in *Solid State Physics*, edited by H. Ehrenreich and D. Turnbull (Academic Press, Boston, 1992), Vol. 46, p. 148-270.
2. M. I. Stockman, S. V. Faleev, and D. J. Bergman, *Anderson Localization vs. Delocalization of Surface Plasmons in Nanosystems: Can One State Have Both Characteristics Simultaneously?*, Phys. Rev. Lett. **87**, 167401-1-4 (2001).
3. M. I. Stockman, D. J. Bergman, and T. Kobayashi, *Coherent Control of Nanoscale Localization of Ultrafast Optical Excitation in Nanosystems*, Phys. Rev. B. **69**, 054202-1-10 (2004).



# Quasistatic Field Equations and Boundary Conditions

$$\frac{\partial}{\partial \mathbf{r}} \varepsilon(\mathbf{r}, \omega) \frac{\partial}{\partial \mathbf{r}} \varphi(\mathbf{r}) = 0, \quad \varphi(x, y, 0) = 0, \quad \varphi(x, y, L_z) = 1,$$

$$\left. \frac{\partial}{\partial x} \varphi(x, y, z) \right|_{x=0, L_x} = \left. \frac{\partial}{\partial y} \varphi(x, y, z) \right|_{y=0, L_y} = 0.$$

Material properties of the system is convenient to express in terms of the spectral parameter

$$s(\omega) = \left( 1 - \frac{\epsilon_m(\omega)}{\epsilon_d(\omega)} \right)^{-1}$$

**Field Equation**

$$\left[ \frac{\partial}{\partial \mathbf{r}} \theta(\mathbf{r}) \frac{\partial}{\partial \mathbf{r}} - s(\omega) \frac{\partial^2}{\partial \mathbf{r}^2} \right] \varphi(\mathbf{r}; \omega) = 0$$

$\theta(\mathbf{r}) = 1$  in metal,  $\theta(\mathbf{r}) = 0$  in dielectric

Physical surface plasmons are elementary excitation whose complex frequency can be found from an equation  $s(\omega_n + i\gamma_n) = s_n$ ,

where the spectral parameter  $s(\omega) = \left(1 - \frac{\epsilon_{\text{metal}}(\omega)}{\epsilon_{\text{host}}(\omega)}\right)^{-1}$

## Retarded Green's function

$$\left[ \frac{\partial}{\partial \mathbf{r}} \theta(\mathbf{r}) \frac{\partial}{\partial \mathbf{r}} - s(\omega) \frac{\partial^2}{\partial \mathbf{r}^2} \right] G^r(\mathbf{r}, \mathbf{r}'; \omega) = \delta(\mathbf{r} - \mathbf{r}')$$

Local fields on nanoscale for harmonic excitation with external field  $\varphi_0(\mathbf{r}, \omega)$  at frequency  $\omega$ :

$$\varphi(\mathbf{r}, \omega) = \varphi_0(\mathbf{r}, \omega) - \int \varphi_0(\mathbf{r}', \omega) \nabla_{\mathbf{r}'} \theta(\mathbf{r}') \nabla_{\mathbf{r}'} G(\mathbf{r}, \mathbf{r}'; \omega) d^3 r',$$

Local fields on nanoscale for short-pulse excitation with pulse field  $\varphi_0(\mathbf{r}, t)$

$$\varphi(\mathbf{r}, t) = \varphi_0(\mathbf{r}, t) - \int \varphi_0(\mathbf{r}', t') \nabla_{\mathbf{r}'} \theta(\mathbf{r}') \nabla_{\mathbf{r}'} G(\mathbf{r}, \mathbf{r}'; t - t') d^3 r' dt',$$

**Eigenmode problem** (homogeneous equations; dependent only on geometry, material independent!)

$$\frac{\partial}{\partial \mathbf{r}} \theta(\mathbf{r}) \frac{\partial}{\partial \mathbf{r}} \varphi_n(\mathbf{r}) = s_n \frac{\partial^2}{\partial \mathbf{r}^2} \varphi_n(\mathbf{r}),$$

where  $\theta(\mathbf{r} \in \text{metal}) = 1$  and  $\theta(\mathbf{r} \in \text{dielectric}) = 0$  ;

$$\varphi_n(x, y, 0) = \varphi_n(x, y, L_z) = 0 ,$$

and

$$\left. \frac{\partial}{\partial x} \varphi_n(x, y, z) \right|_{x=0, L_x} = \left. \frac{\partial}{\partial y} \varphi_n(x, y, z) \right|_{y=0, L_y} = 0 .$$

In terms of the eigenmodes, Green's function spectral expansion is very simple

$$G^r(\mathbf{r}, \mathbf{r}'; \omega) = \sum_n \frac{\varphi_n(\mathbf{r}) \varphi_n^*(\mathbf{r}')}{s(\omega) - s_n}$$

Irrespectively of the precision with which the eigenfunctions and eigenvalues are found (as long as the eigenfunction are properly orthonormal and the eigenvalues satisfy the corresponding sum rule, this Green's function *exactly* satisfies the general requirements of the theory due to its correct analytical structure.

In particular, it has only simple poles in the lower half-plane of complex frequency. Thus it satisfies Kramers-Kronig causality relations.

The poles of this Green's function describe SP plasmon modes. The resonant (singular) part of the Green's function is

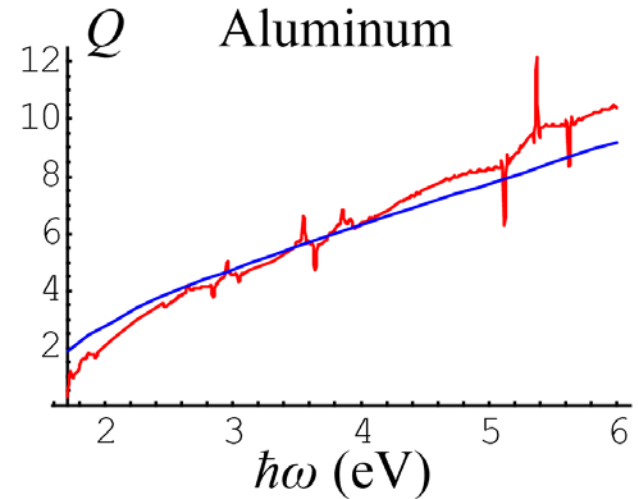
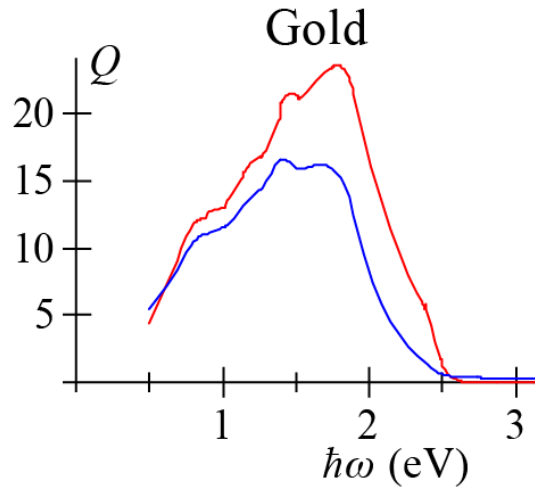
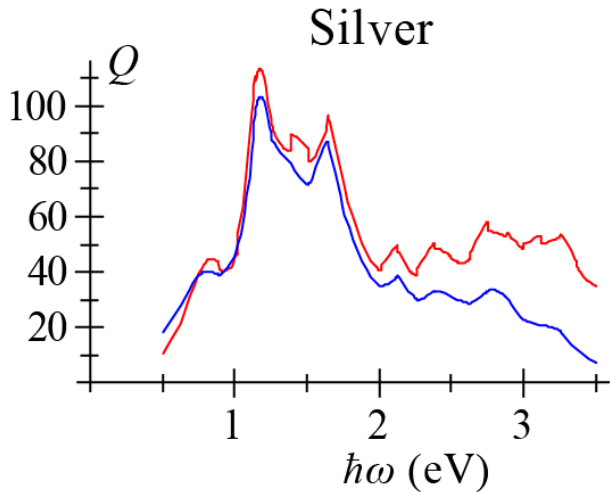
$$G^r(\mathbf{r}', \mathbf{r}; \omega) = \frac{1}{s'(\omega_n)} \sum_n \frac{\phi_n^*(\mathbf{r}') \phi_n(\mathbf{r})}{\omega - \omega_n + i\gamma_n}; \quad s(\omega_n) = s_n; \quad \gamma_n = \left. \frac{\text{Im } \varepsilon_m}{\omega \frac{\partial \text{Re } \varepsilon_m}{\partial \omega}} \right|_{\omega=\omega_n}$$

At a resonant pole, the Green's function and local fields are increased by the plasmonic quality factor,

$$Q = \frac{\omega}{2\gamma} = \frac{\omega \frac{\partial \text{Re } \varepsilon_m}{\partial \omega}}{2 \text{Im } \varepsilon_m}$$

$$E_\alpha(\mathbf{r}, \omega) = E_\alpha^{(0)}(\mathbf{r}, \omega) + \int \frac{\partial^2 G^r(\mathbf{r}, \mathbf{r}'; \omega)}{\partial r_\alpha \partial r'_\beta} E_\beta^{(0)}(\mathbf{r}', \omega) d^3 r'$$

## Quality Factor of SP Resonances



$$Q = \frac{\omega}{2\gamma} \approx \frac{\omega \frac{\partial \text{Re} \epsilon_m(\omega)}{\partial \omega}}{2 \text{Im} \epsilon_m(\omega)}$$

$$Q = \frac{-\text{Re} \epsilon_m(\omega)}{\text{Im} \epsilon_m(\omega)}$$

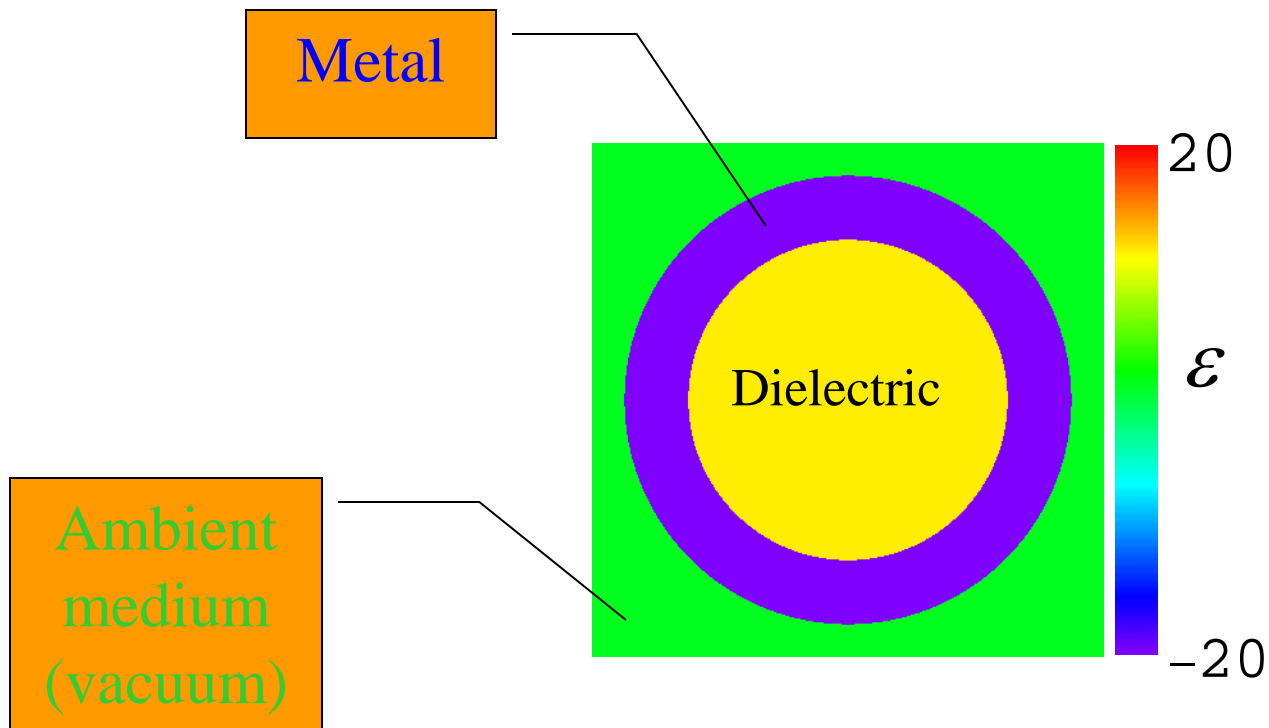
Exact

Simplified

These two definitions coincide for the extreme Drude case:  $\epsilon_m = -\frac{\omega_p^2}{\omega^2}$



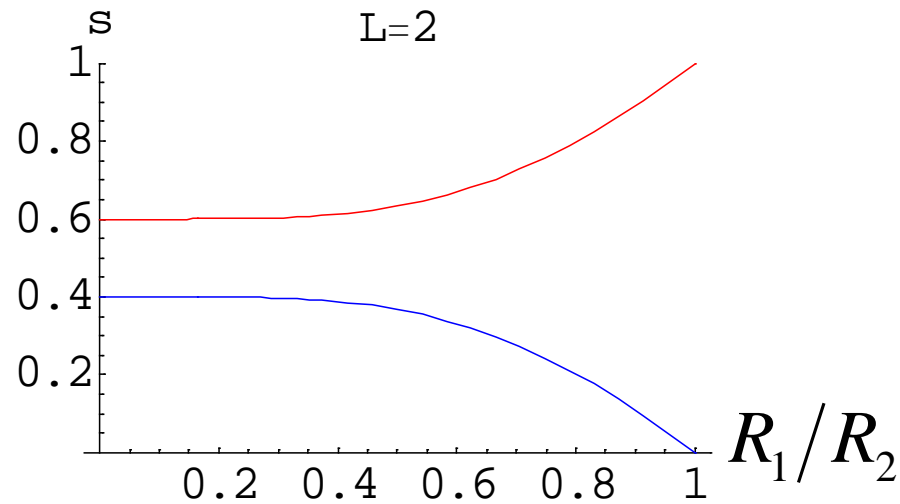
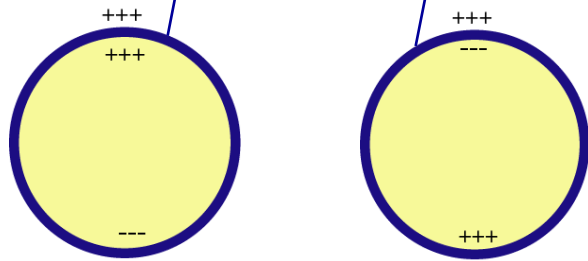
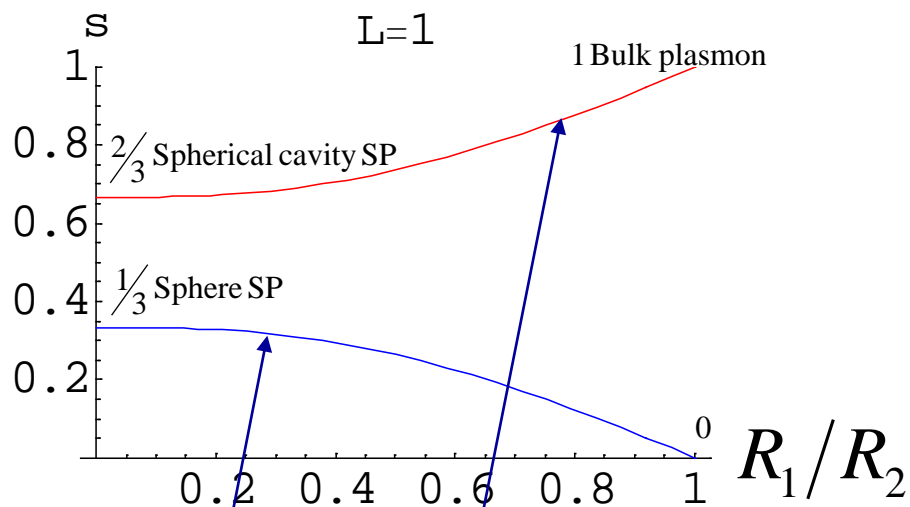
# Nanoshells



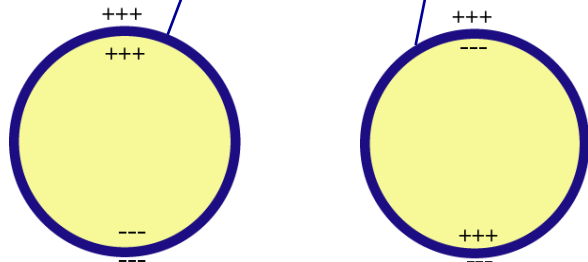
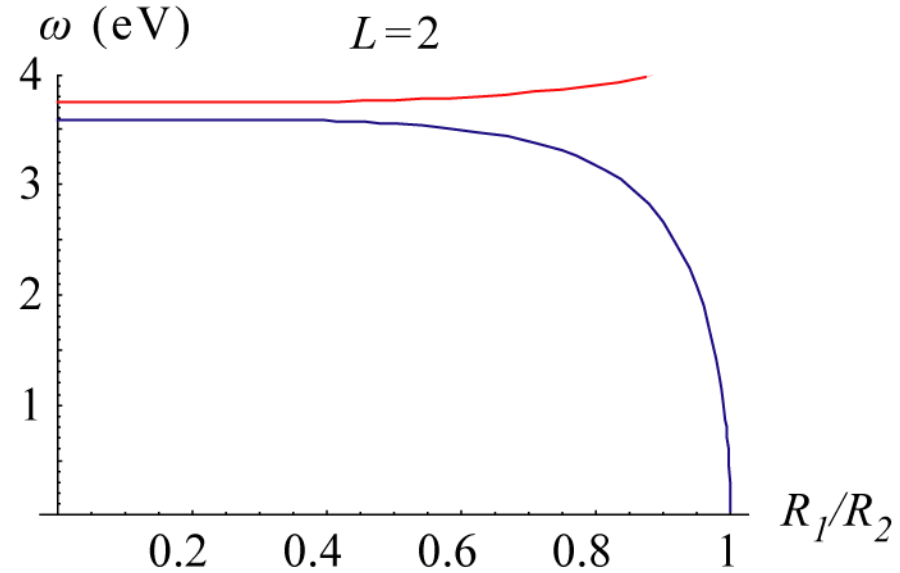
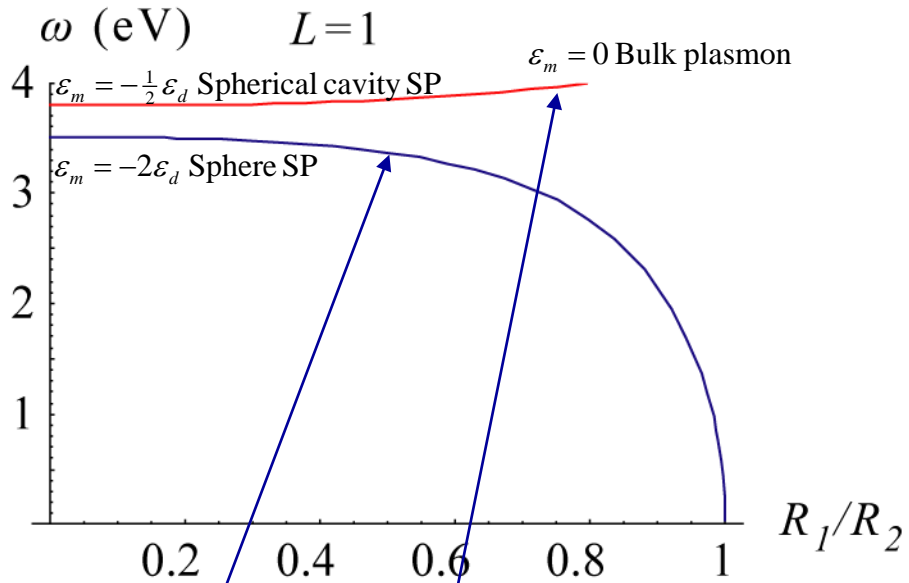
1. S. J. Oldenburg, R. D. Averitt, S. L. Westcott, and N. J. Halas, *Nanoengineering of Optical Resonances*, Chem. Phys. Lett. **288**, 243-247 (1998).
2. R. D. Averitt, S. L. Westcott, and N. J. Halas, *Linear Optical Properties of Gold Nanoshells*, J Opt Soc Am B **16**, 1824-1832 (1999).
3. S. J. Oldenburg, J. B. Jackson, S. L. Westcott, and N. J. Halas, *Infrared Extinction Properties of Gold Nanoshells*, Appl. Phys. Lett. **75**, 2897-2899 (1999).
4. S. J. Oldenburg, S. L. Westcott, R. D. Averitt, and N. J. Halas, *Surface Enhanced Raman Scattering in the near Infrared Using Metal Nanoshell Substrates*, J. Chem. Phys. **111**, 4729-4735 (1999).
5. S. L. Westcott, S. J. Oldenburg, T. R. Lee, and N. J. Halas, *Construction of Simple Gold Nanoparticle Aggregates with Controlled Plasmon-Plasmon Interactions*, Chem. Phys. Lett. **300**, 651-655 (1999).
6. S. L. Westcott, J. B. Jackson, C. Radloff, and N. J. Halas, *Relative Contributions to the Plasmon Line Shape of Metal Nanoshells*, Phys. Rev. B **66**, - (2002).
7. L. R. Hirsch, R. J. Stafford, J. A. Bankson, S. R. Sershen, B. Rivera, R. E. Price, J. D. Hazle, N. J. Halas, and J. L. West, *Nanoshell-Mediated near-Infrared Thermal Therapy of Tumors under Magnetic Resonance Guidance*, Proc. Natl. Acad. Sci. USA **100**, 13549-13554 (2003).  
L. R. Hirsch, J. B. Jackson, A. Lee, N. J. Halas, and J. West, *A Whole Blood Immunoassay Using Gold Nanoshells*, Anal Chem **75**, 2377-2381 (2003).
9. D. P. O'Neal, L. R. Hirsch, N. J. Halas, J. D. Payne, and J. L. West, *Photo-Thermal Tumor Ablation in Mice Using near Infrared-Absorbing Nanoparticles*, Cancer Lett **209**, 171-176 (2004).
10. C. L. Nehl, N. K. Grady, G. P. Goodrich, F. Tam, N. J. Halas, and J. H. Hafner, *Scattering Spectra of Single Gold Nanoshells*, Nano Lett. **4**, 2355 -2359 (2004).
10. C. Loo, A. Lowery, N. Halas, J. West, and R. Drezek, *Immunotargeted Nanoshells for Integrated Cancer Imaging and Therapy*, Nano Lett. **5**, 709-711 (2005).
11. C. E. Talley, J. B. Jackson, C. Oubre, N. K. Grady, C. W. Hollars, S. M. Lane, T. R. Huser, P. Nordlander, and N. J. Halas, *Surface-Enhanced Raman Scattering from Individual Au Nanoparticles and Nanoparticle Dimer Substrates*, Nano Lett. **5**, 1569-1574 (2005).

Eigenvalues of plasmon eigenmodes (resonances)  
(Material independent)

$$s_{L\pm} = \frac{1}{2} \left[ 1 \pm \frac{1}{2L+1} \sqrt{1 + 4L(L+1) \left( \frac{R_1}{R_2} \right)^{2L+1}} \right]$$



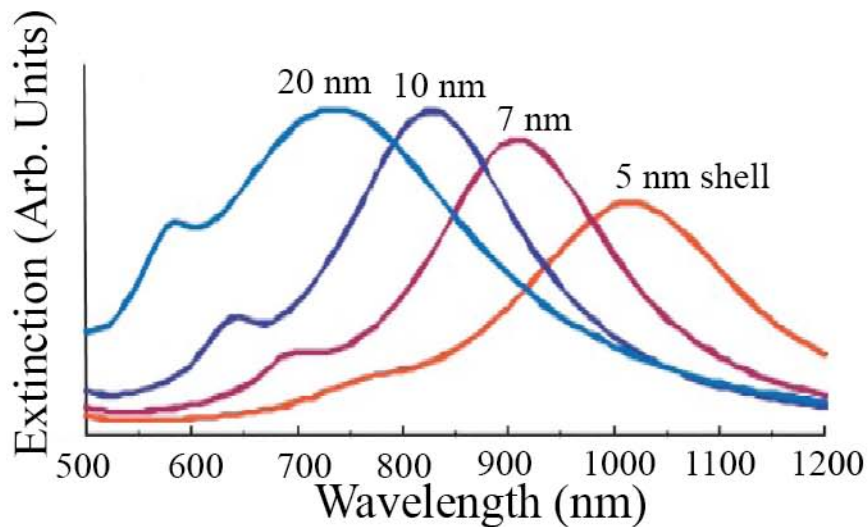
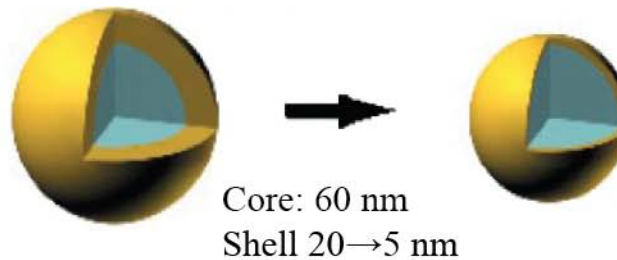
# Eigenfrequencies of Surface Plasmons for Silver



Aspect ratio:  $R_1 / R_2$

J. L. West and N. J. Halas, *Engineered Nanomaterials for Biophotonics Applications: Improving Sensing, Imaging, and Therapeutics*, *Annu. Rev. Biomed. Eng.*, 5, 285-292 (2003).

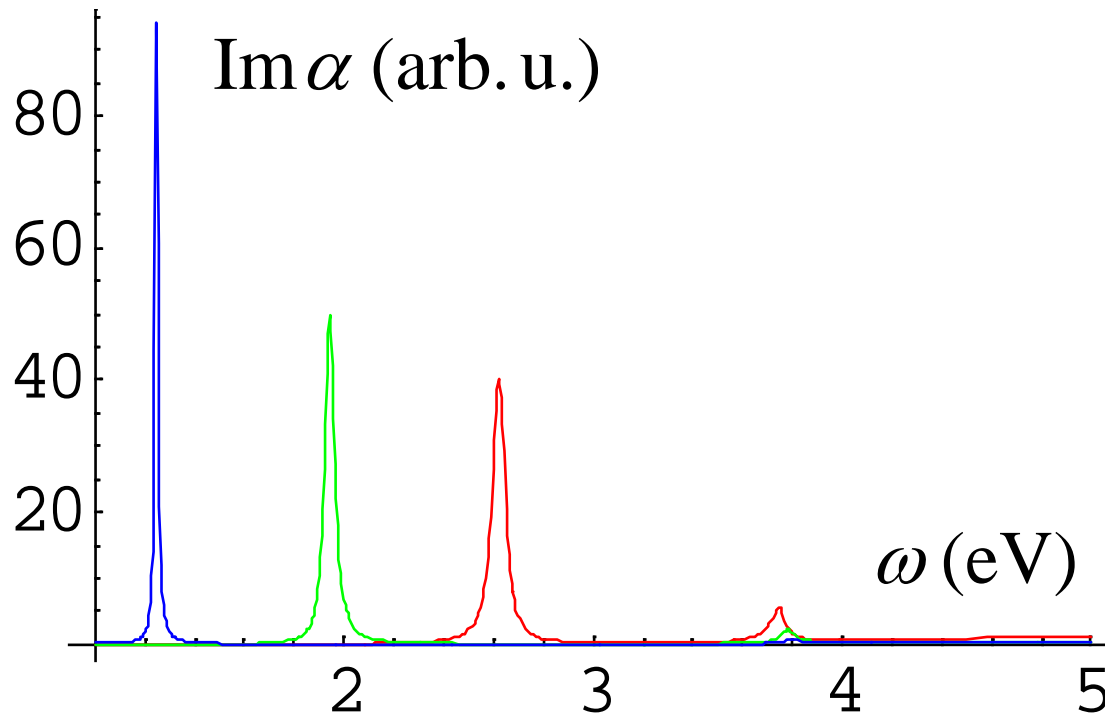
# Nanoshell Spectral Properties



# Absorption Cross Section of Silver Nanoshells

$$\sigma = 2\pi \frac{\omega}{c} \text{Im } \alpha$$

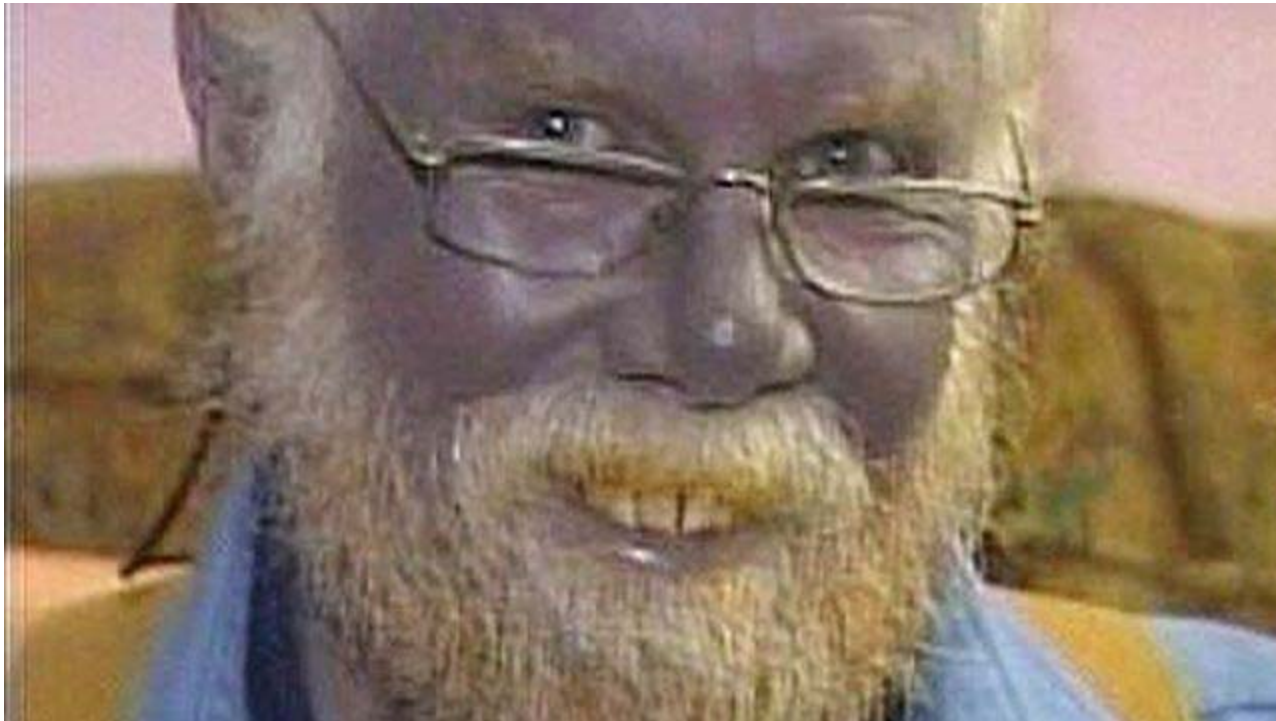
$$R_1:R_2 = 20:30, 25:30, 28:30$$



Gold is biologically inert. Colloidal gold can be consumed in macroscopic amounts without long-time damage.

In contrast, colloidal silver is very and irreversibly toxic.

This man drank colloidal silver. He is dead at 61.





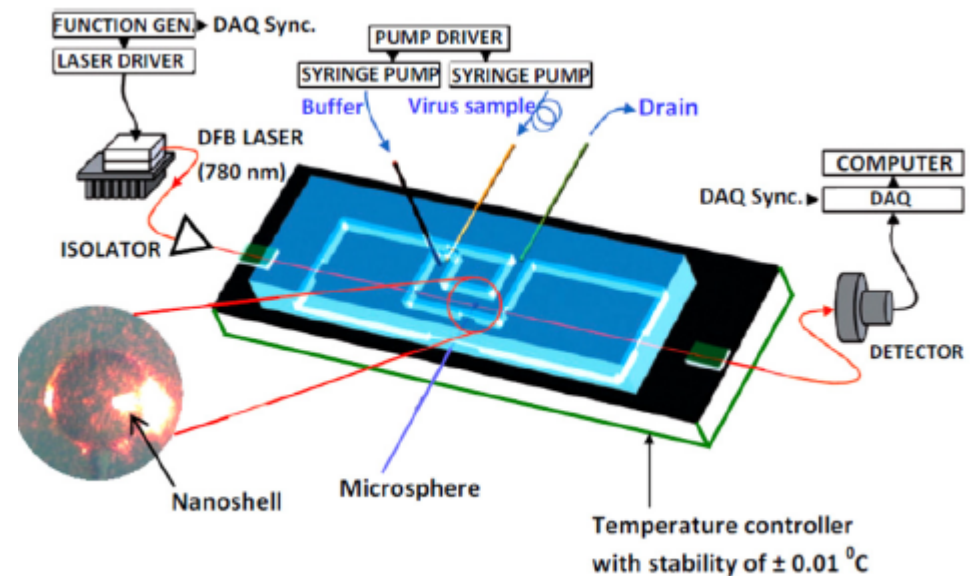
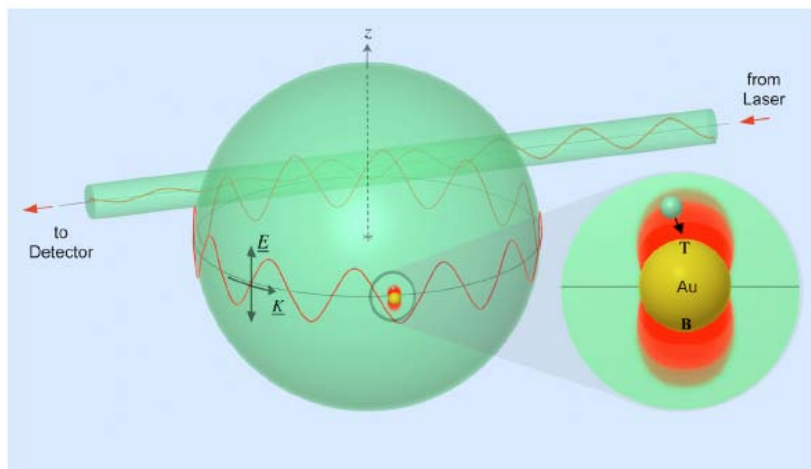
APPLIED PHYSICS LETTERS **101**, 043704 (2012)

## Taking whispering gallery-mode single virus detection and sizing to the limit

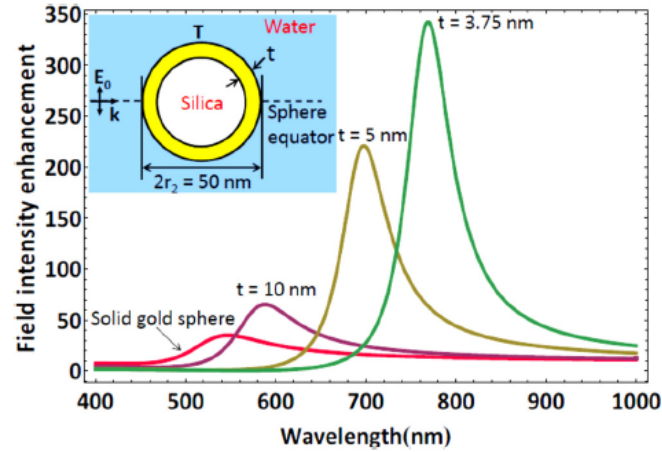
V. R. Dantham,<sup>1</sup> S. Holler,<sup>1,2</sup> V. Kolchenko,<sup>3</sup> Z. Wan,<sup>4</sup> and S. Arnold<sup>1,a</sup>

<sup>1</sup>Microparticle Photophysics Lab, Polytechnic Institute of NYU, Brooklyn, New York 11201, USA

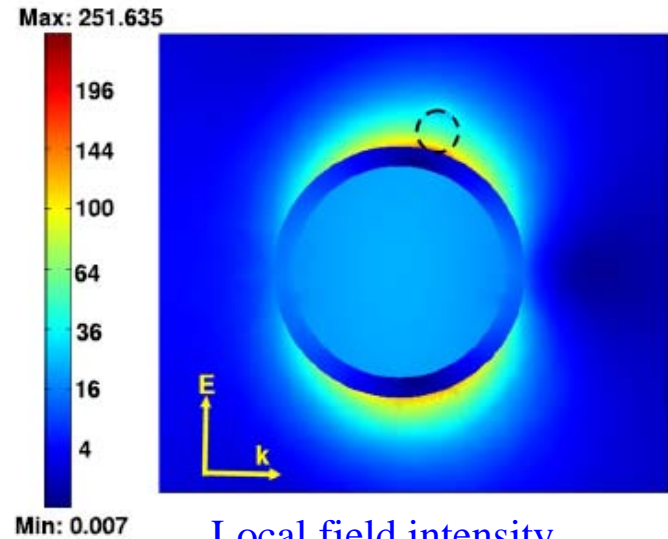
We report the label-free detection and sizing by a microcavity of the smallest individual RNA virus, MS2, with a mass only  $\sim 1\%$  of InfluenzaA (6 vs. 512 ag). Although detection of such a small bio-nano-particle has been beyond the reach of a bare spherical microcavity, it was accomplished with ease ( $S/N=8$ ,  $Q=4 \times 10^5$ ) using a single dipole stimulated plasmonic-nanoshell as a microcavity wavelength shift enhancer, providing an enhancement of  $\sim 70\times$ , in agreement with theory. Unique wavelength shift statistics are recorded consistent with an ultra-uniform genetically programmed substance that is drawn to the plasmonic hot spots by light-forces. © 2012 American Institute of Physics. [<http://dx.doi.org/10.1063/1.4739473>]







Nanoshell spectra



Local field intensity

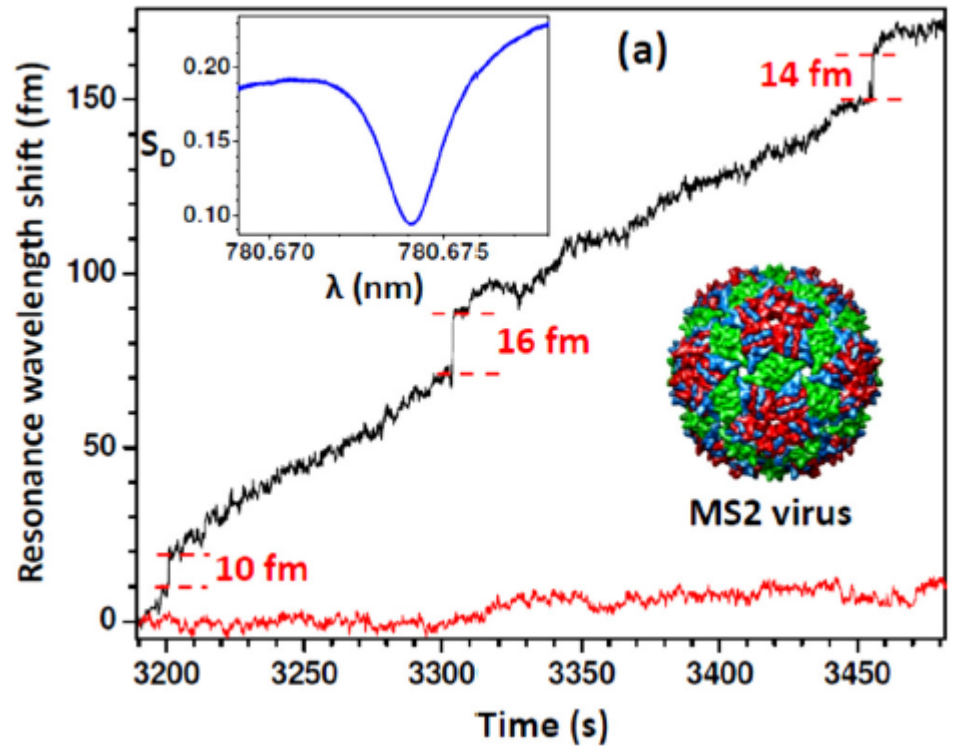


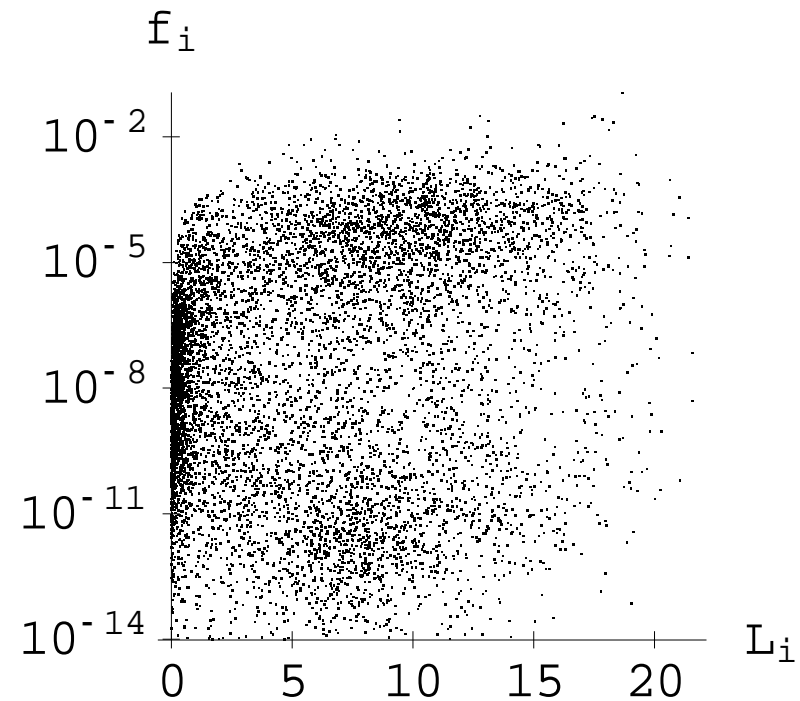
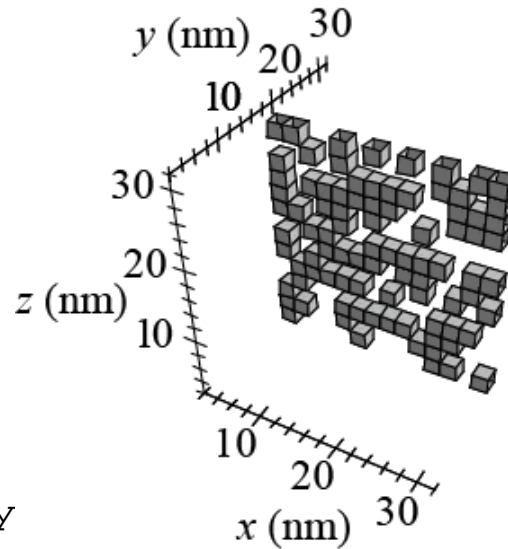
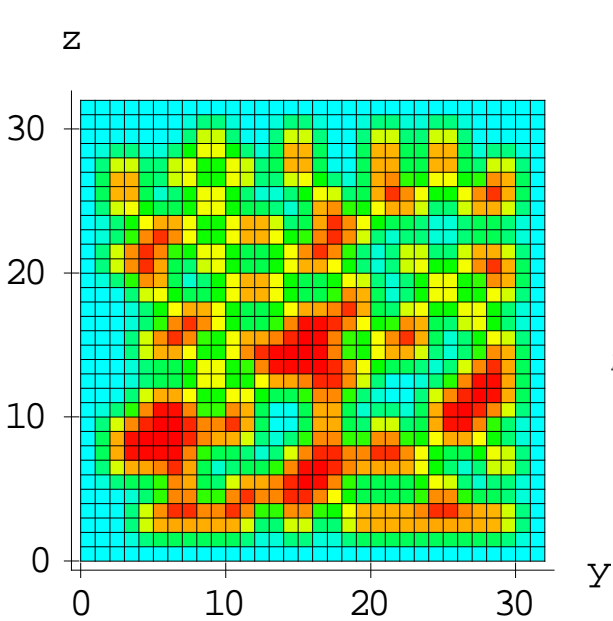
FIG. 3. (a) Shift of resonance wavelength above 780.674 nm of a WGM resonator  $R = 45 \mu\text{m}$  having a gold nanoshell attached at its equator due to the adsorption of MS2 viruses (upper trace). The lower trace shows the background without MS2 or the gold nanoshell (r.m.s. noise 2 fm). Insets show the recorded spectrum  $S_D$  for the hybrid resonator ( $Q \sim 4 \times 10^5$ ) and an illustration of MS2 virus (radius  $a \sim 13.6$  nm). (b) Step number statistics for all

# Localization of Surface Plasmons

**Any Anderson-localized (or, strongly localized) mode is dark.**

Consequently:

**It is impossible that all surface-plasmon modes of any system are Anderson-localized (or, strongly localized).**



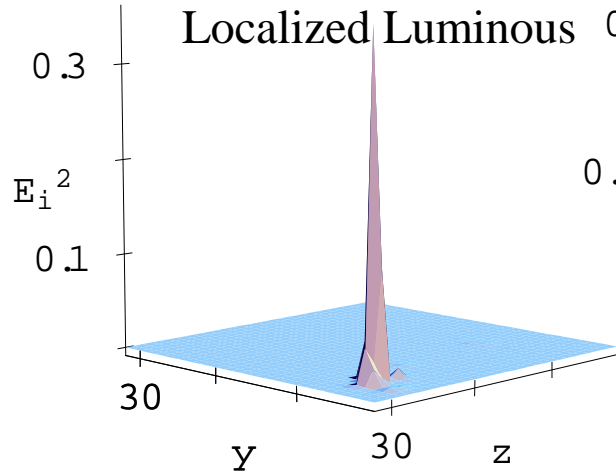
## Geometry of Random Planar Composite

Distribution of Eigenmodes over their Oscillator Strength  $f_i$  and Localization Radius  $L_i$

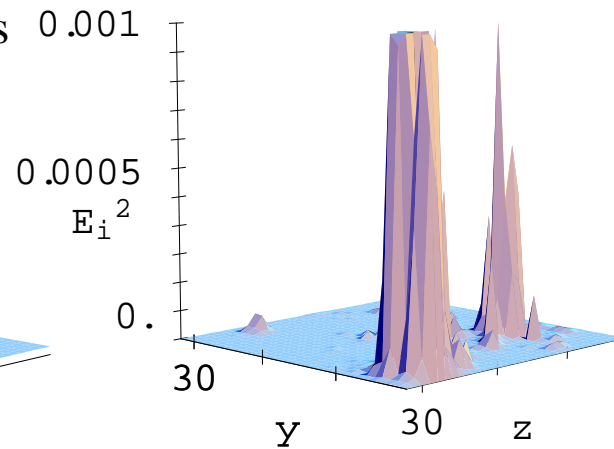
Phys. Rev. Lett. **87**, 167401 (2001).

# Local Field Intensities for Four Eigenmodes Representative of Each Class of Eigenmodes

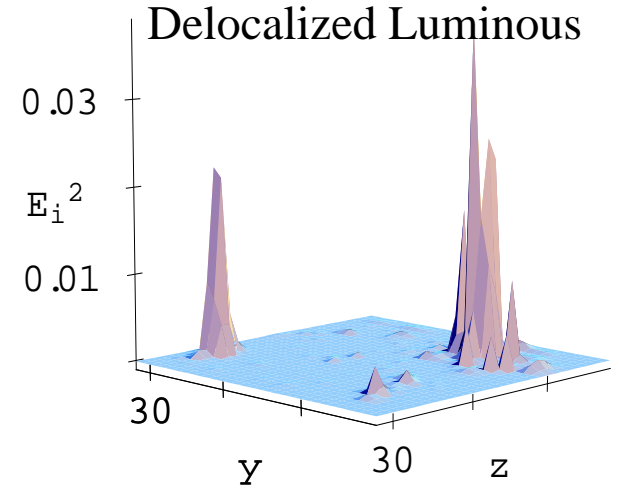
$s_i=0.1995$  ,  $L_i=2.1$



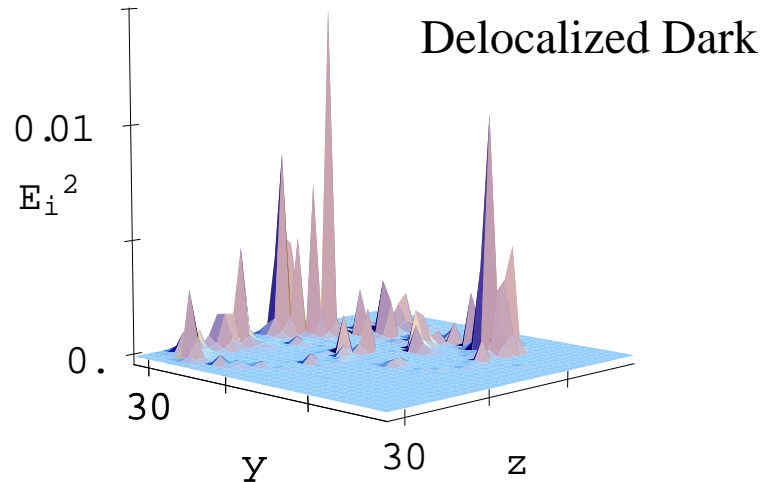
$s_i=0.1995$  ,  $L_i=2.1$



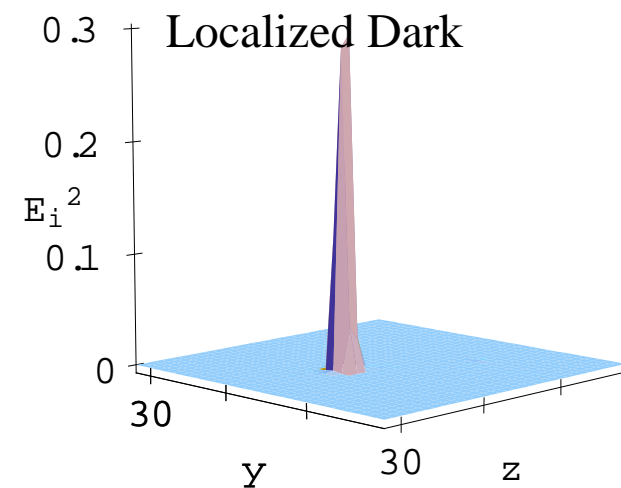
$s_i=0.2$  ,  $L_i=11.2$



$s_i=0.201$  ,  $L_i=9.6$

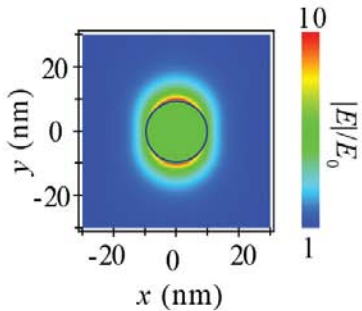


$s_i=0.2015$  ,  $L_i=1.$

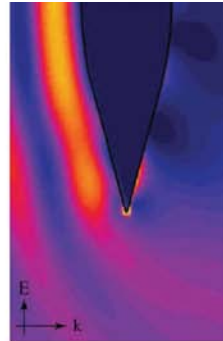


# Plasmonic Near-Field **Hot Spots**: Happy 16<sup>th</sup> Anniversary!

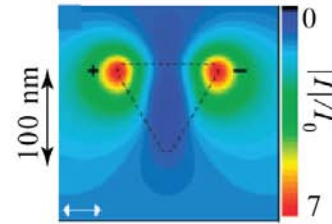
• M. I. Stockman et al., *Phys. Rev. Lett.* **75**, 2450 (1995)



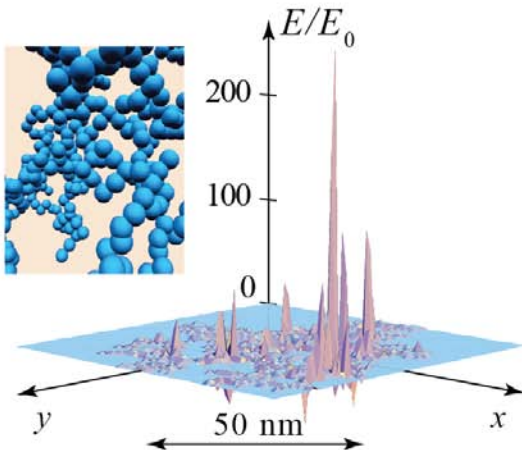
Silver nanosphere



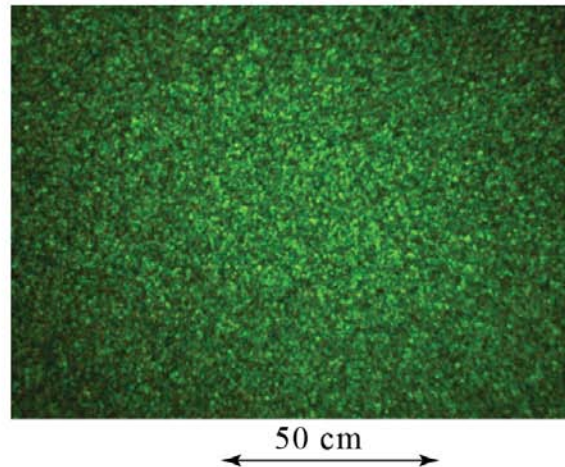
Metal tip: L. Novotny and S. J. Stranick, *Annual Rev. Phys. Chem.* **57**, 303-331 (2006)



Nano-pyramid: M. Rang et al., *Nano Lett.* **8**, 3357 (2008)



Fractal cluster of silver: M. I. Stockman, L. N. Pandey, and T. F. George, *Phys. Rev. B* **53**, 2183-2186 (1996)



Optical counterpart: laser speckles on a screen

$$R_{\text{Speckle}} \sim \frac{\lambda}{A} L$$

$R_{\text{Speckle}}$  is speckle size

$\lambda \sim 100$  nm is reduced wave length

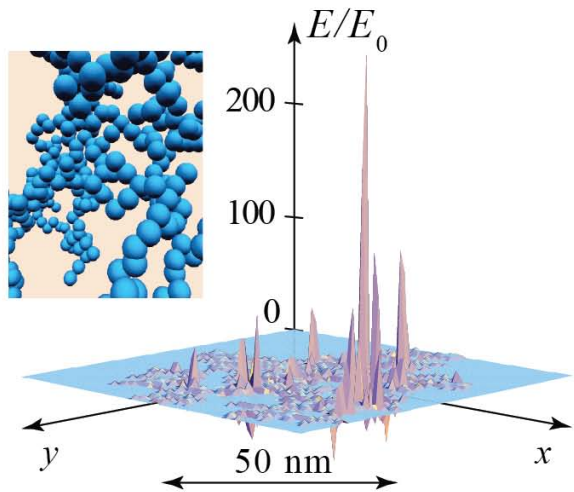
$A$  is laser spot size,

$L$  is distance to the screen

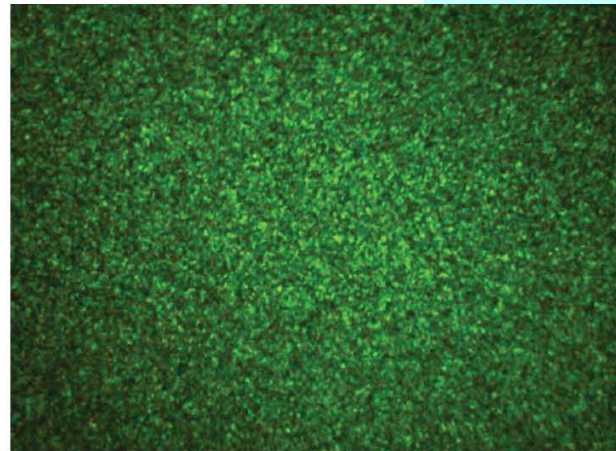


# Plasmonic Near-Field Hot Spots: Happy 20<sup>th</sup> Anniversary!

- D. P. Tsai et al., *Phys. Rev. Lett.* **72**, 4149 (1994).
- M. I. Stockman et al., *Phys. Rev. Lett.* **75**, 2450 (1995)
- M. I. Stockman, L. N. Pandey, and T. F. George, *Phys. Rev. B* **53**, 2183 (1996)



M. I. Stockman, L. N. Pandey, and T. F. George, *Phys. Rev. B* 53, 2183 (1996).



50 cm  
Random scattering speckles

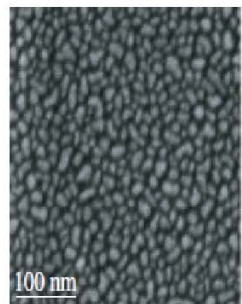
$$R_{\text{Speckle}} \sim \frac{\hat{\lambda}}{A} L$$

$R_{\text{Speckle}}$  is speckle size

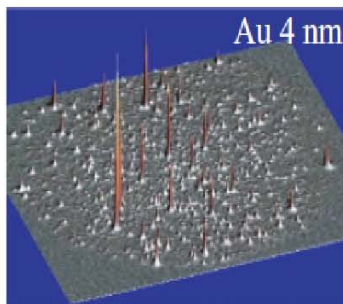
$\hat{\lambda} \sim 100$  nm is reduced wave length

$A$  is laser spot size,

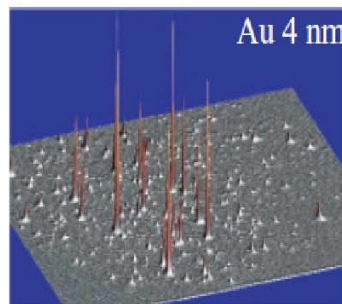
$L$  is distance to the screen



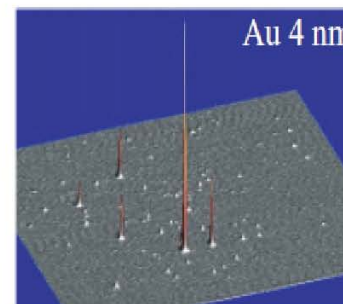
Au 4 nm,  $f = 0.53$



$\lambda = 800$  nm, Hot Spots Nb = 617



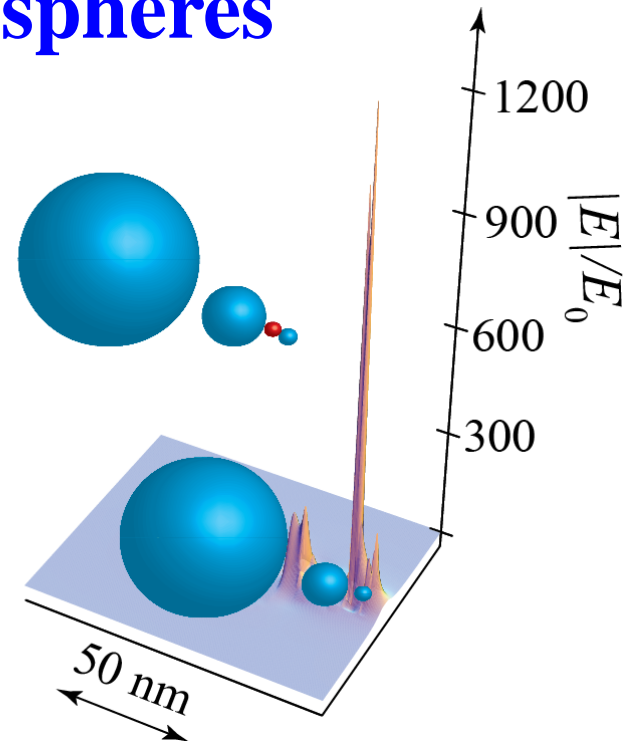
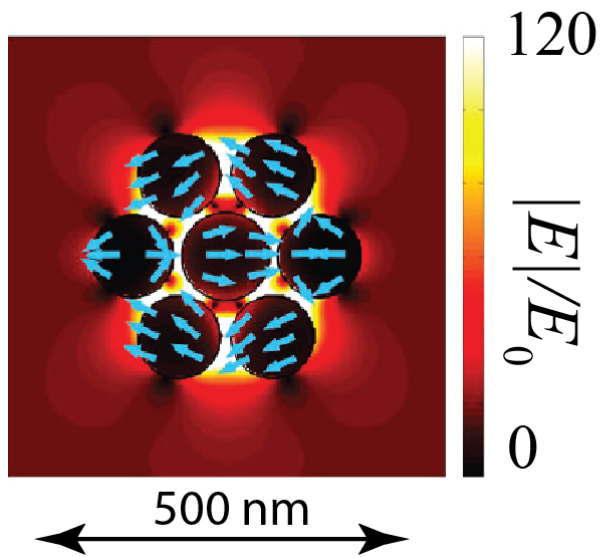
$\lambda = 930$  nm, Hot Spots Nb = 453



$\lambda = 970$  nm, Hot Spots Nb = 402

C. Awada, G. Barbillon, F. Charra, L. Douillard, and J. J. Greffet, *Phys. Rev. B* **85**, 045438 (2012).

# Engineered Nanoplasmonic Hot Spots in Small Clusters of Nanospheres



Fano resonance in a nanosphere cluster:

- J. A. Fan et al., *Science* **328**, 1135 (2010)
- M. Hentschel et al., *Nano Lett.* **10**, 2721 (2010)

Self-similar nanosphere nanolens: K. Li, M. I. Stockman, and D. J. Bergman, *Phys. Rev. Lett.* **91**, 227402 (2003)

# Giant Raman Scattering in Complex Natural and Engineered Nanosystems

## Theory of SERS (Surface Enhanced Raman Scattering)

1. M. I. Stockman, V. M. Shalaev, M. Moskovits, R. Botet, and T. F. George, *Enhanced Raman Scattering by Fractal Clusters: Scale Invariant Theory*, Phys. Rev. B **46**(5), 2821-2830 (1992).
2. M. I. Stockman, *Electromagnetic Theory of SERS*, in: Springer Series Topics in Applied Physics, edited by K. Kneipp, M. Moskovits and H. Kneipp, *Surface Enhanced Raman Scattering – Physics and Applications* (Springer-Verlag, Heidelberg New York Tokyo, 2006).



## Discovery of Surface Enhanced Raman Scattering (SERS)

1. M. Fleischmann, P. J. Hendra, and A. J. McQuillan, *Raman Spectra of Pyridine Adsorbed at a Silver Electrode*, Chem. Phys. Lett. **26**, 163-166 (1974).
2. D. L. Jeanmaire and R. P. Van Duyne, *Surface Raman Spectroelectrochemistry Part I. Heterocyclic, Aromatic, and Aliphatic Amines Adsorbed on the Anodized Silver Electrode*, J. Electroanal. Chem. **84**, 1-20 (1977).
3. M. G. Albrecht and J. A. Creighton, *Anomalously Intense Raman Spectra of Pyridine at a Silver Electrode*, J. Amer. Chem. Soc. **99**, 5215 - 5217 (1977).

Raman scattering from molecules absorbed on clusters of colloidal silver or rough silver surfaces enhanced by a factor of  $G^{RS} \sim 10^4 - 10^6$  with respect to the same molecules free in solution

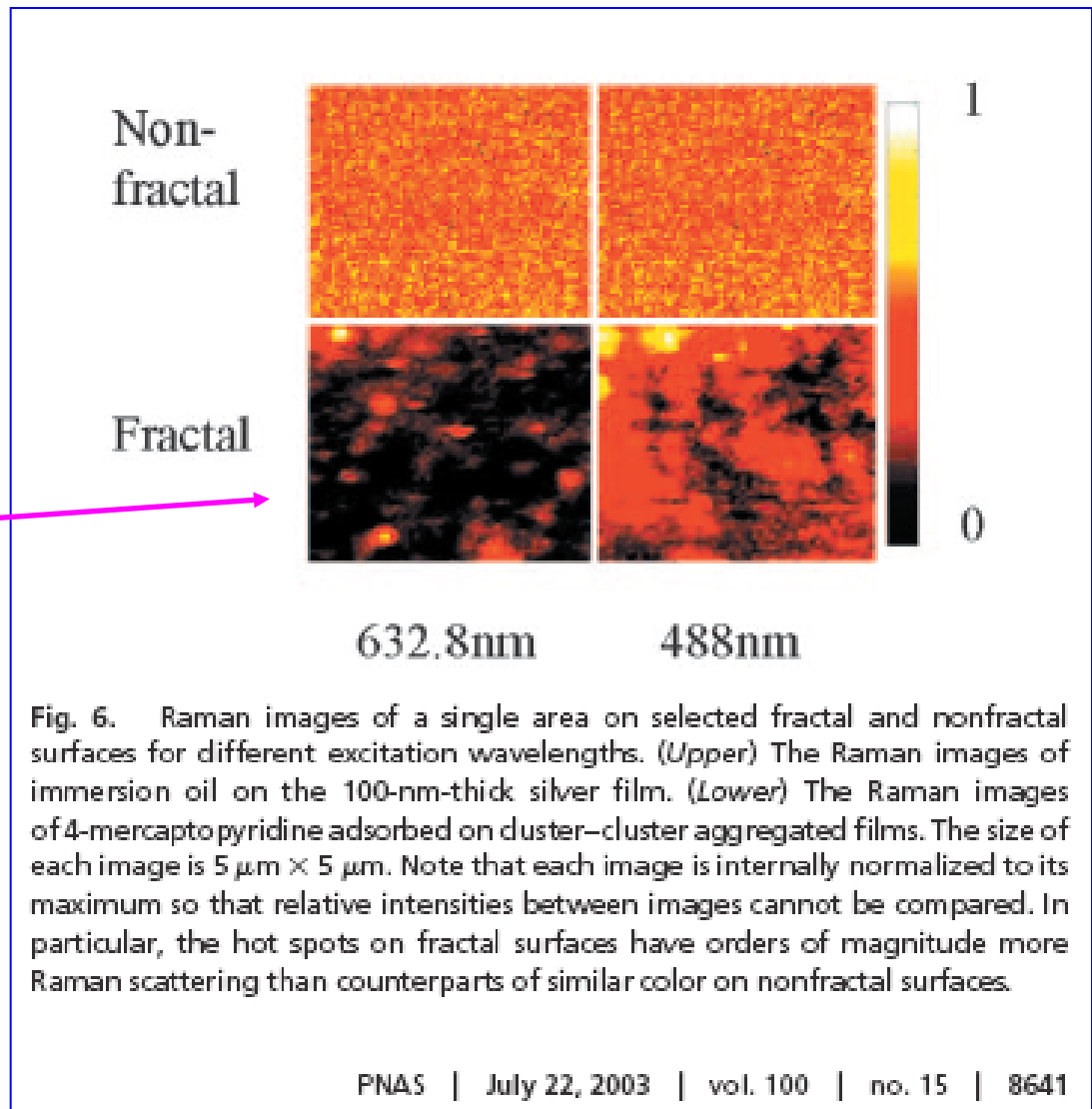
Observation of Single-molecule Surface-Enhanced Raman  
Scattering:

•K. Kneipp, Y. Wang, H. Kneipp, L. T. Perelman, I. Itzkan, R. Dasari, and M. S. Feld, *Single Molecule Detection Using Surface-Enhanced Raman Scattering (SERS)*, Phys. Rev. Lett. **78**, 1667-1670 (1997).

•S. M. Nie and S. R. Emery, *Probing Single Molecules and Single Nanoparticles by Surface-Enhanced Raman Scattering*, Science **275**, 1102-1106 (1997).

See also: Z. J. Wang, S. L. Pan, T. D. Krauss, H. Du, and L. J. Rothberg, *The Structural Basis for Giant Enhancement Enabling Single-Molecule Raman Scattering*, Proc. Natl. Acad. Sci. USA **100**, 8638-8643 (2003).

SERS enhanced by  
 a factor  $10^{12} - 10^{14}$



## A Frequency Domain Existence Proof of Single-Molecule Surface-Enhanced Raman Spectroscopy

Jon A. Dieringer, Robert B. Lettan II, Karl A. Scheidt, and Richard P. Van Duyne\*

Northwestern University, Department of Chemistry, 2145 Sheridan Road,  
Evanston, Illinois 60208

J. AM. CHEM. SOC. 2007, 129, 16249–16256

**Scheme 1.** Chemical Structure of the Two Isotopologues, R6G- $d_4$  and R6G- $d_0$

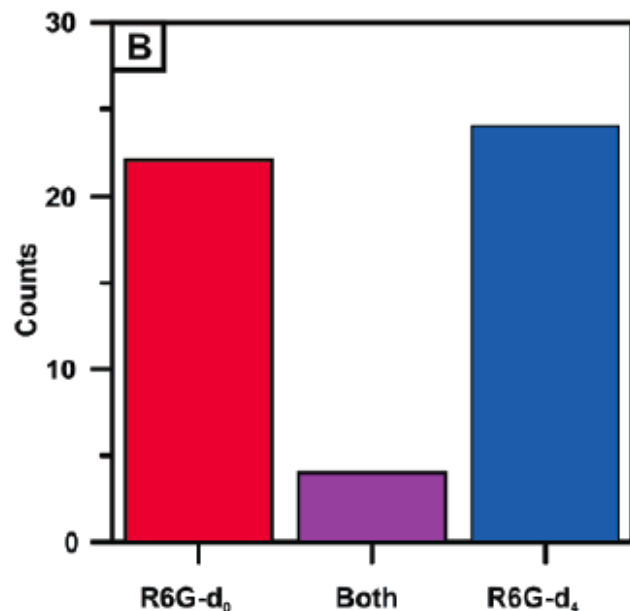
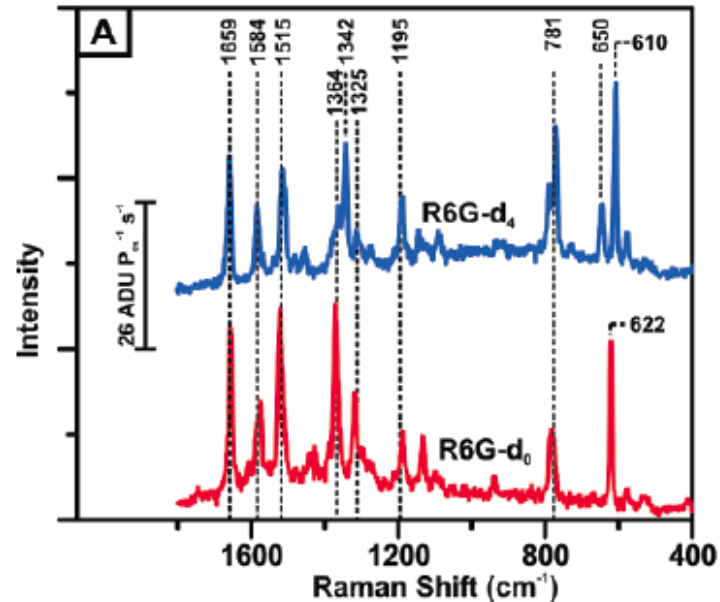
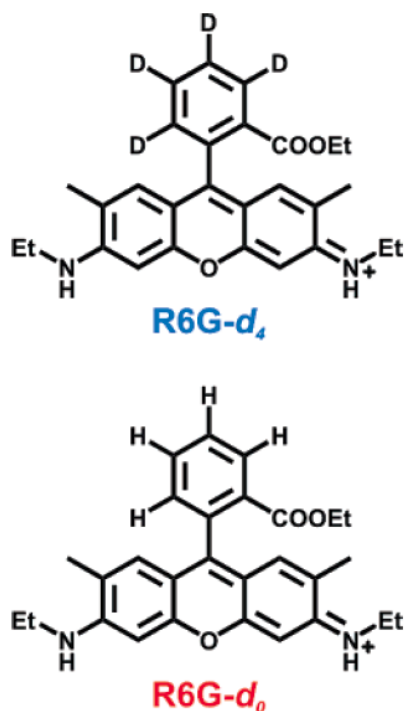
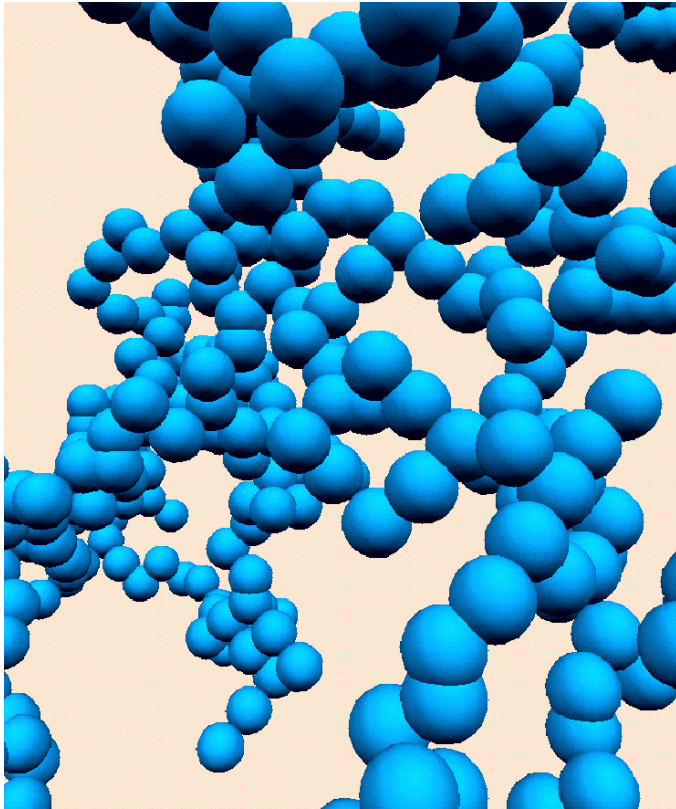
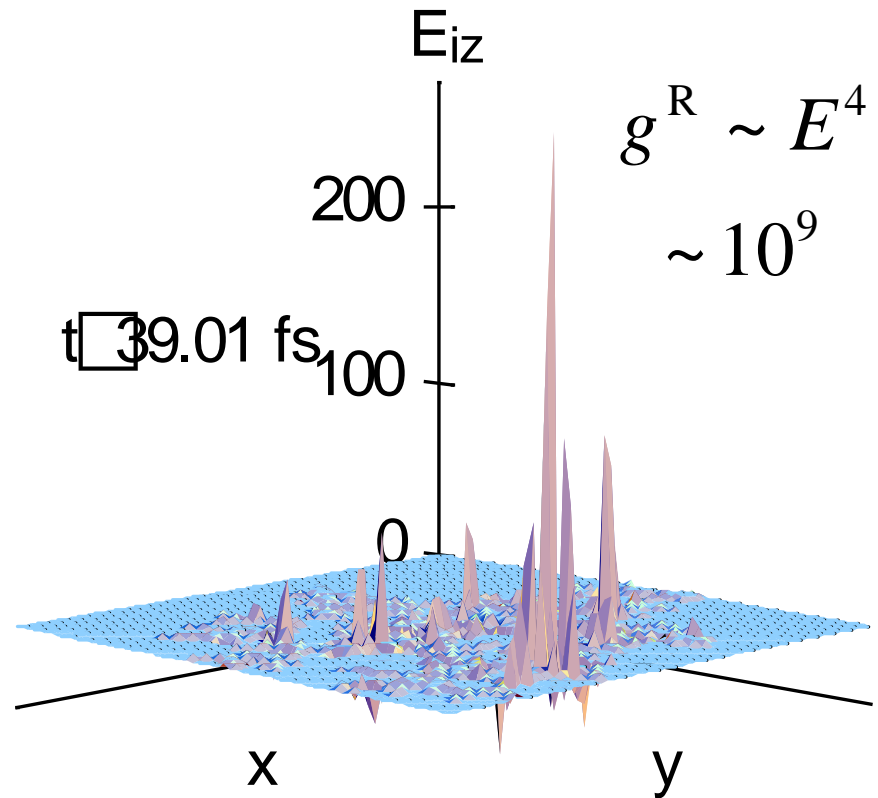


**Figure 2.** (A) Two representative spectra from the single-molecule results where one contains uniquely R6G- $d_0$  (red line) and the other uniquely R6G- $d_4$  (blue line) vibrational character. ( $\lambda_{\text{ex}} = 532 \text{ nm}$ ,  $t_{\text{aq}} = 10 \text{ s}$ ,  $P_{\text{ex}} = 2.4 \text{ W/cm}^2$ , grazing incidence) (B) Histogram detailing the frequency with which only R6G- $d_0$ , only R6G- $d_4$  and both R6G- $d_0$  and R6G- $d_4$  vibrational modes were observed with low adsorbate concentration under dry  $\text{N}_2$  environment.

## Enhancement of Optical Responses in Fractals

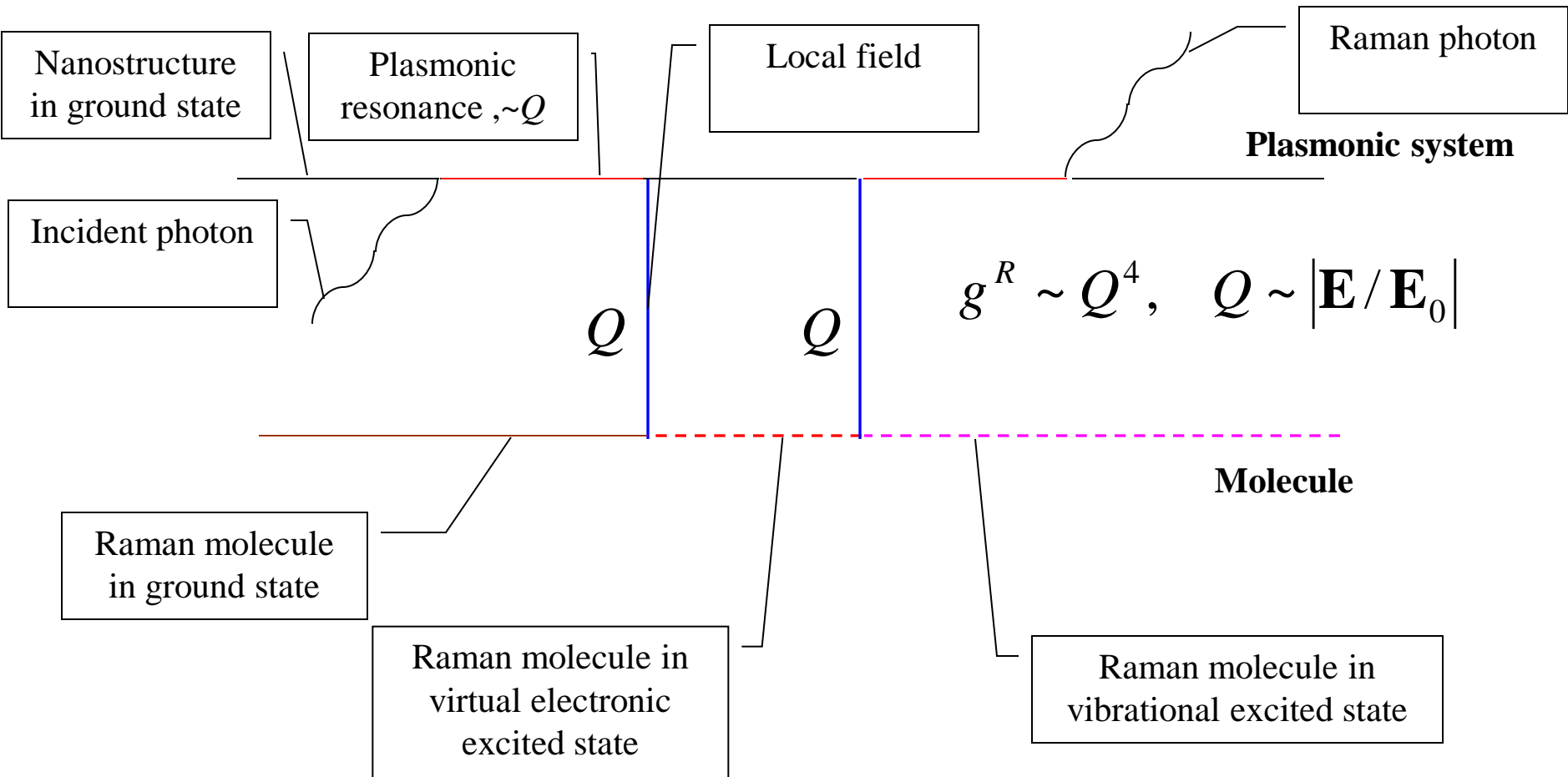


Self-similar fractal geometry

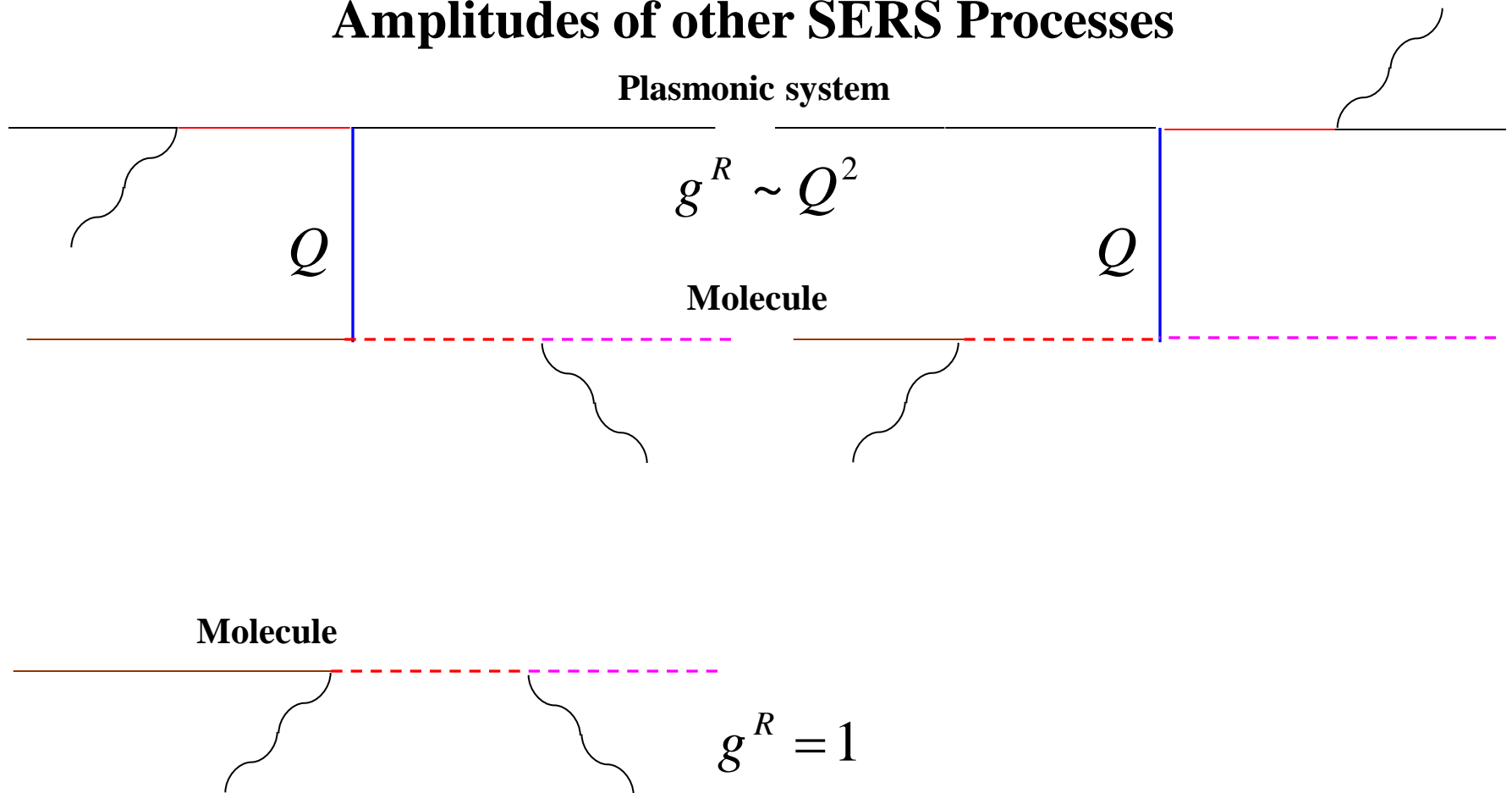


Local optical fields in fractal cluster [MIS, Phys. Rev. Lett. **84**, 1011 (2000) ].

## Amplitude of the Leading SERS Process



## Amplitudes of other SERS Processes



Enhancement coefficient of SERS for a molecule at a point  $\mathbf{r}_0$

$$g^R = \frac{1}{|s(\omega_R)|^2} \sum_{\alpha=x,y,z} \left| \sum_{\beta=x,y,z} g_{\beta\alpha}(\mathbf{r}_0; \omega^R) g_{\beta z}(\mathbf{r}_0, \omega) \right|^2$$

$g^R \sim Q^4$

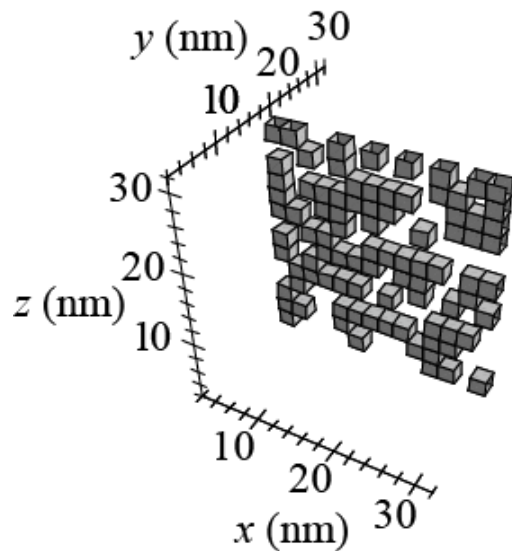
where the local field enhancement factor is expressed in terms of dyadic Green's function

$$g_{\alpha\beta}(\mathbf{r}, \omega) = \int_V G_{\alpha\beta}^r(\mathbf{r}, \mathbf{r}'; \omega) \Theta(\mathbf{r}') d^3 r'$$

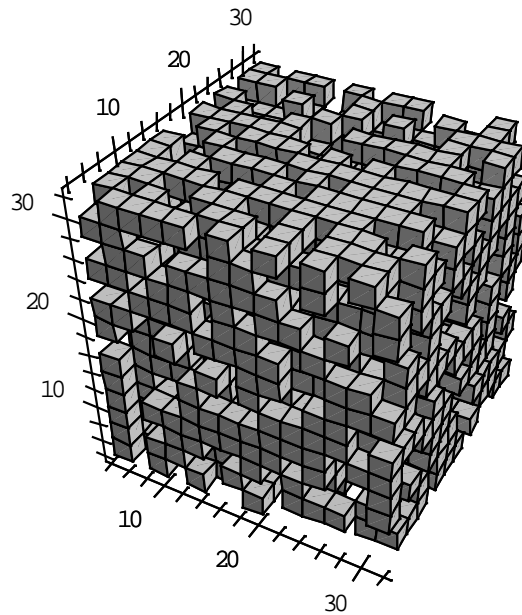
$$G_{\alpha\beta}^r(\mathbf{r}, \mathbf{r}'; \omega) = \frac{\partial^2}{\partial r_\alpha \partial r_\beta} G^r(\mathbf{r}, \mathbf{r}'; \omega)$$



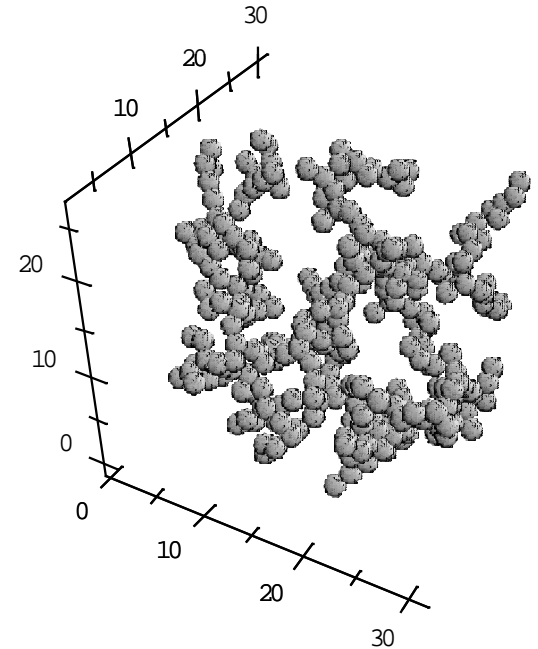
## Types of Systems



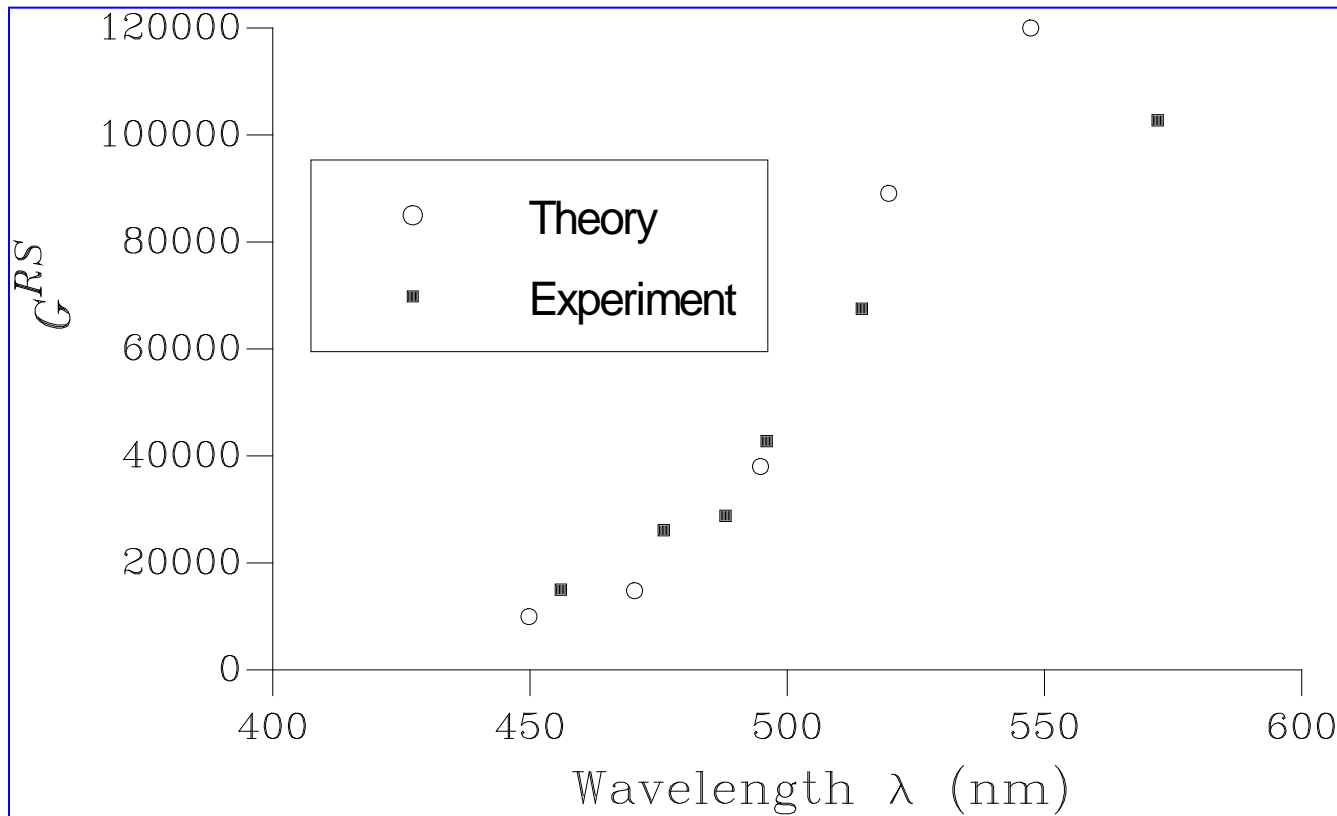
Random Planar Composite



Random Bulk Composite



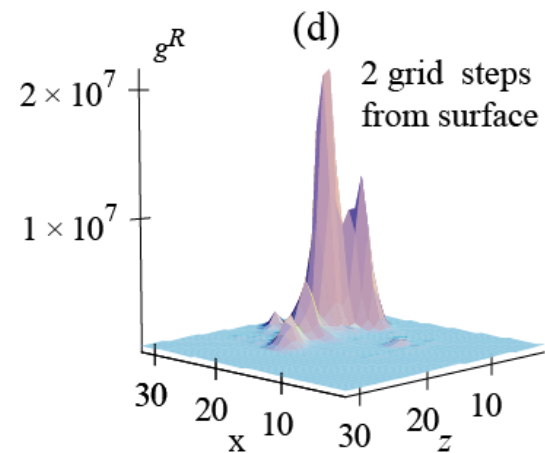
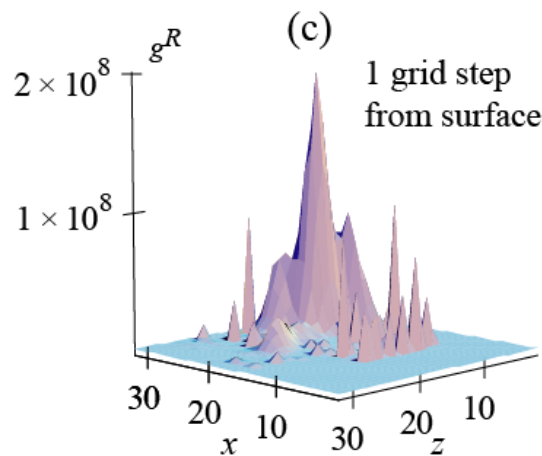
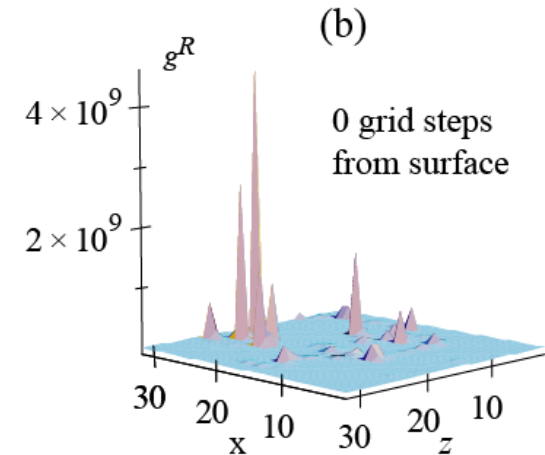
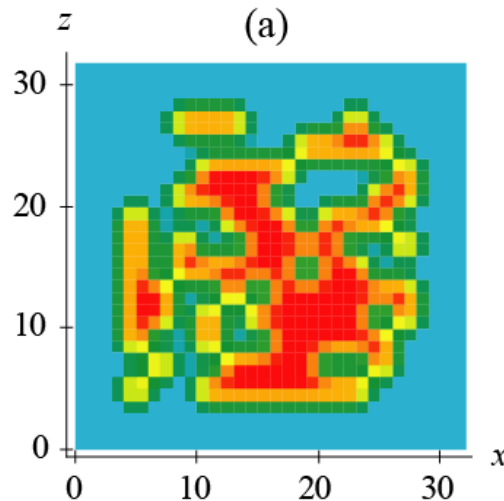
Fractal Cluster (Cluster-Cluster Aggregate)



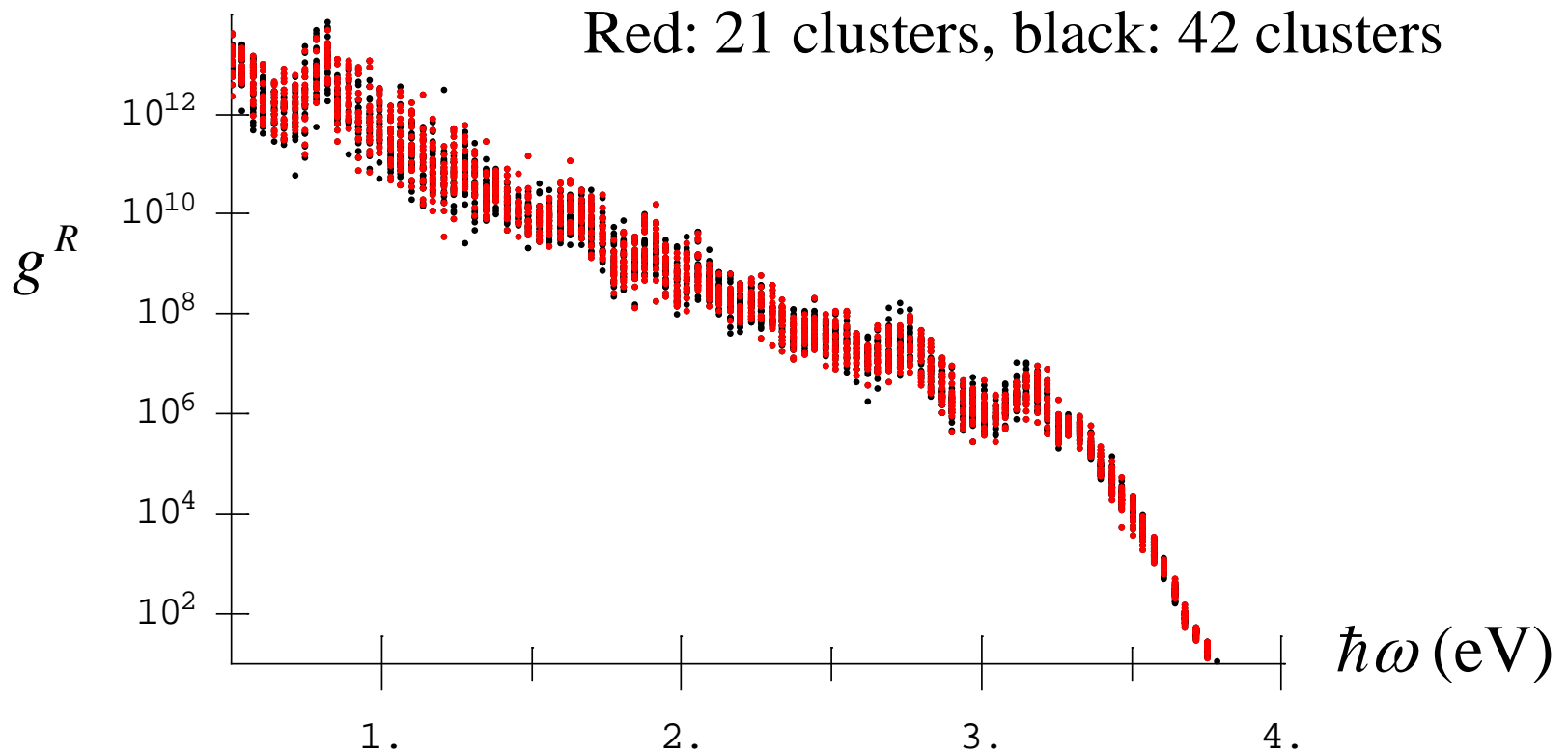
Comparison of theoretical predictions and experimental data for the SERS enhancement coefficient from silver colloid clusters [M. I. Stockman, V. M. Shalaev, M. Moskovits, R. Botet, and T. F. George, *Enhanced Raman-Scattering by Fractal Clusters - Scale-Invariant Theory*, Phys. Rev. B **46**, 2821-2830 (1992)].

Theory: Single molecule  
SERS enhancement for  
different distances from  
rough silver surface

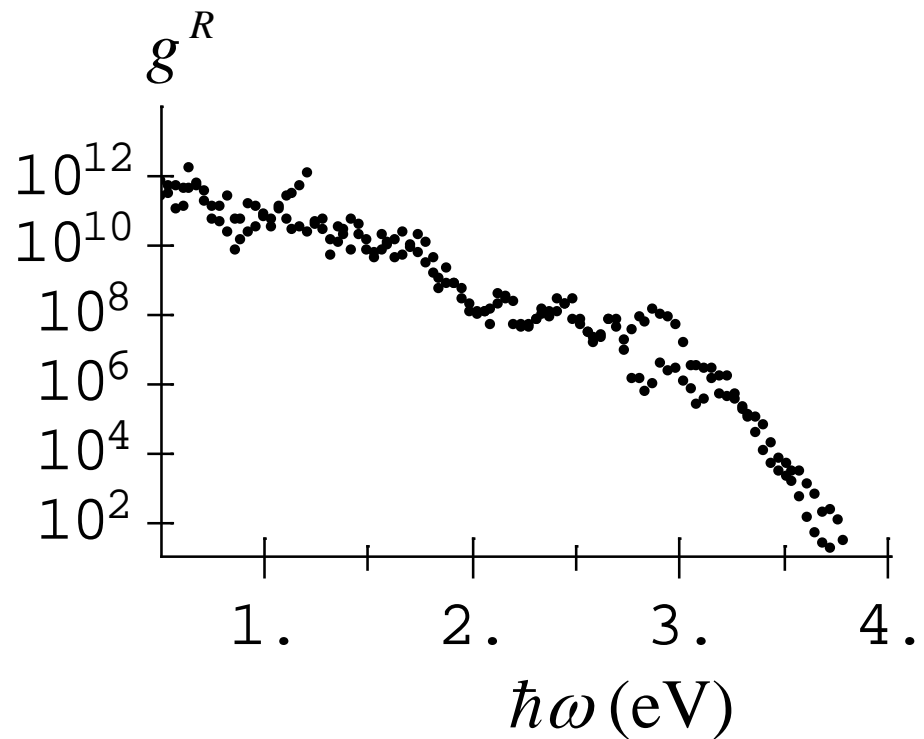
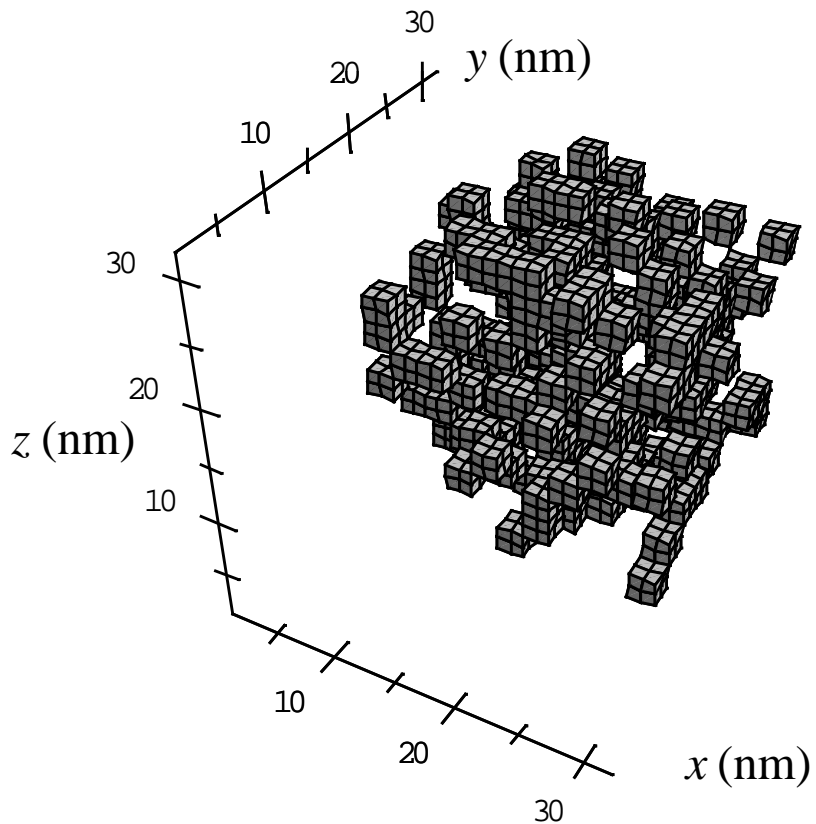
Random Planar  
Composite



Theory: Spectrum of SERS enhancement for a single molecule at silver surface at the “hottest spot” obtained from a large ensemble of systems



## Fractal Cluster (Cluster-Cluster Aggregate)



# A Hybrid Plasmonic–Photonic Nanodevice for Label-Free Detection of a Few Molecules

Francesco De Angelis,<sup>1,†</sup> Maddalena Patrini,<sup>§</sup> Gobind Das,<sup>1,†</sup> Ivan Maksymov,<sup>§</sup>  
Matteo Galli,<sup>§</sup> Luca Businaro,<sup>1</sup> Lucio Claudio Andreani,<sup>§</sup> and Enzo Di Fabrizio<sup>\*,1,†,||</sup>

*BIONEM laboratory, University of Magna Graecia, Campus S. Venuta, Germaneto, viale Europa, 88100 Catanzaro, Italy, CNISM and Department of Physics “A. Volta”, University of Pavia, via Bassi 6, 27100 Pavia, Italy, TASC National Laboratory, CNR-INFN, Area Science Park, Basovizza, 34012 Trieste, Italy, and CalMED s.r.l., Campus S. Venuta, Germaneto, viale Europa, 88100 Catanzaro, Italy*

Received April 18, 2008; Revised Manuscript Received June 6, 2008

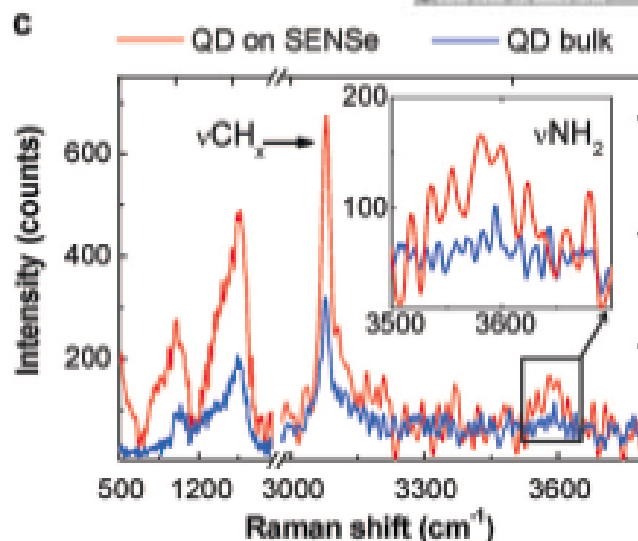
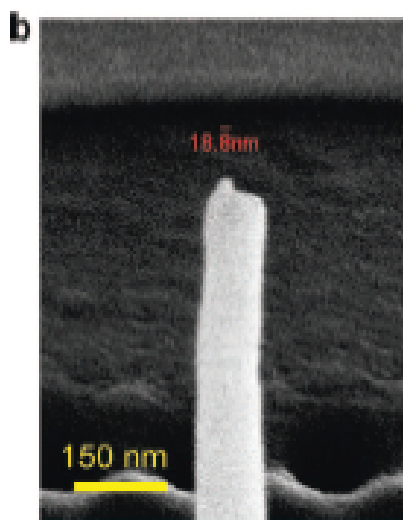
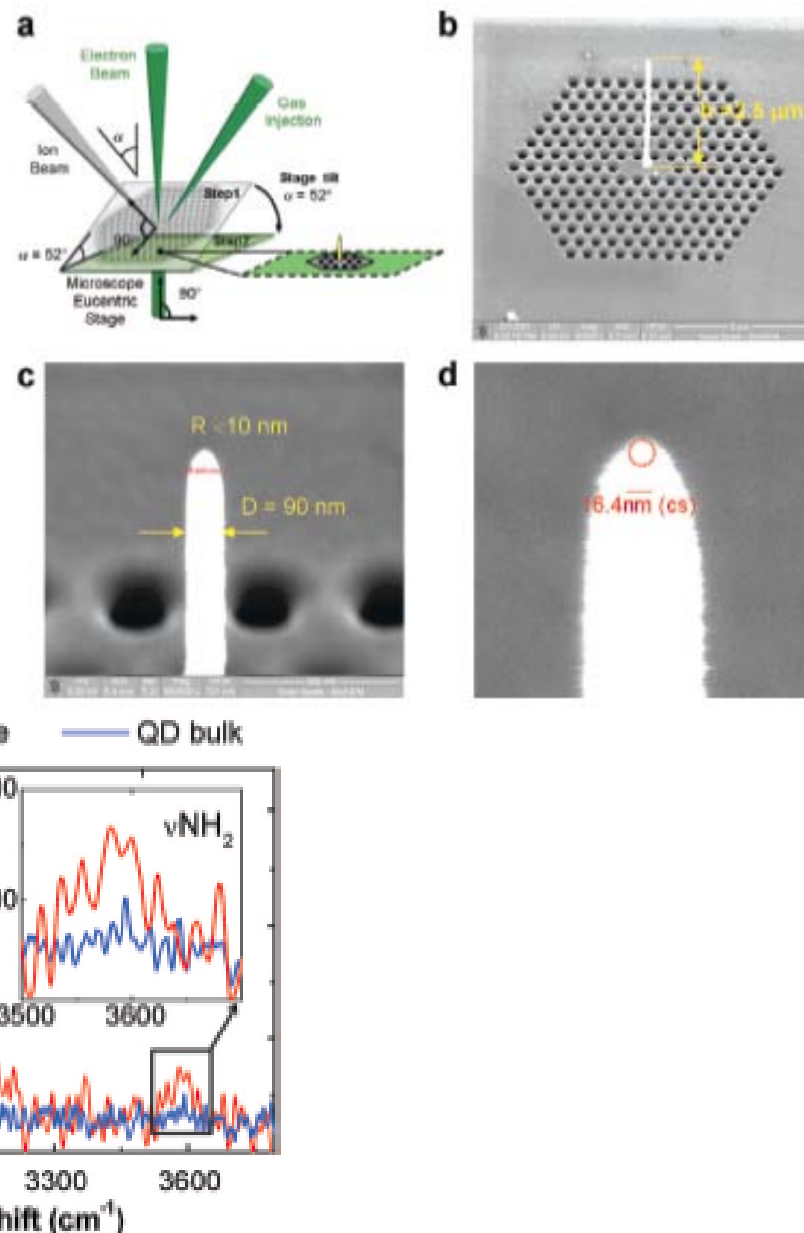


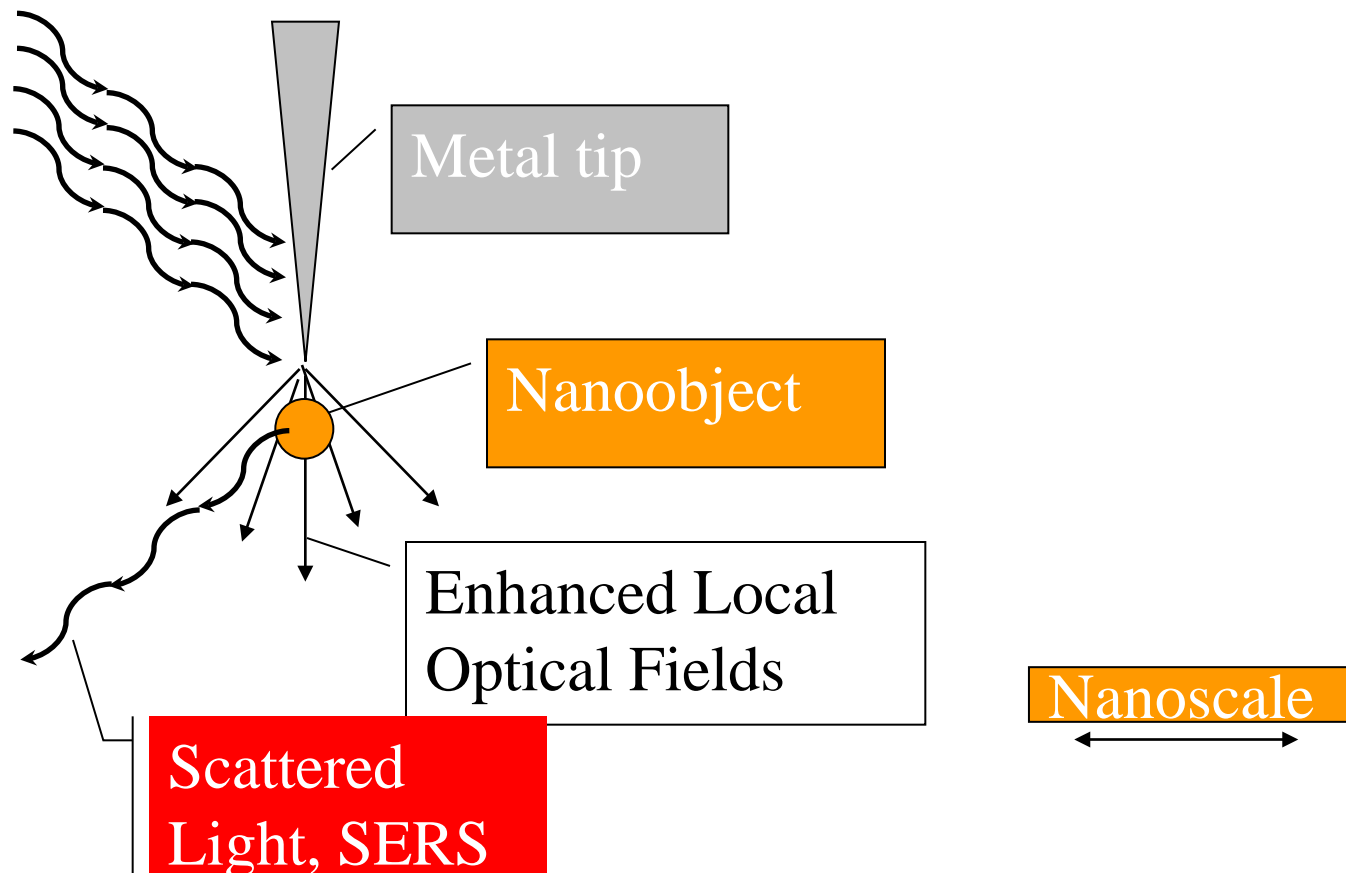
Figure 4. Single quantum dot deposition on the nanoantenna. (a) SEM images arranged in progressive magnification (from top left to bottom right) to show the deposition technique of QDs from the manipulator tip to the nanoantenna. (b) SEM image of a single core–shell ZnS/CdSe QD deposited at the SENSE tip. (c) Raman scattering spectra ( $\lambda_{exc} = 514$  nm,  $P = 0.18$  mW,  $T_{int} = 150$  s) taken from the single QD (red line) as compared to that of a QD bulk sample (blue line). In the inset the asymmetric stretching vibration,  $\nu$ -NH<sub>2</sub>, at  $3580$  cm<sup>-1</sup> is reported in the range between  $3400$  and  $3800$  cm<sup>-1</sup>.

## Conclusions

- Electromagnetic theory of SERS predicts enhancement at 2 eV (600 nm) on order or less than  $10^9$ -  $10^{10}$ , which is three to four orders of magnitude less than experimentally observed
- Theory for random composites and fractal clusters predicts approximately the same magnitude of enhancement\
- Adiabatic concentration in nanoplasmonic tapers provide an alternative and very efficient way to SERS, including SERS nanoscopy
- Other factors must contribute to SERS:

Chemical enhancement? J. Jiang, K. Bosnick, M. Maillard, and L. Brus, *Single Molecule Raman Spectroscopy at the Junctions of Large Ag Nanocrystals*, J. Phys. Chem. B **107**, 9964-9972 (2003)

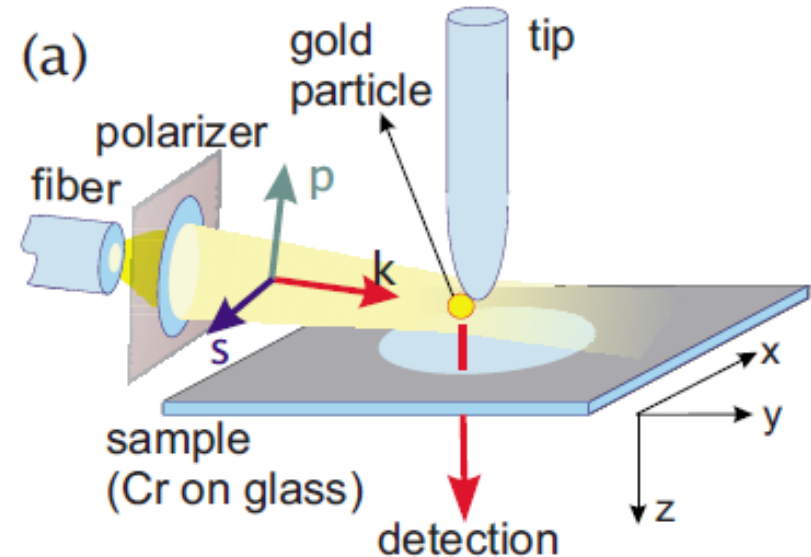
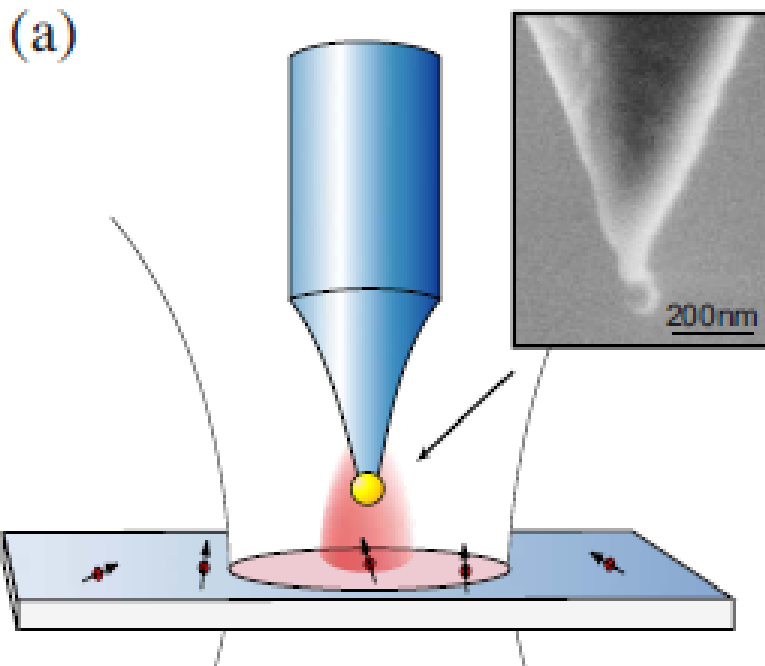
# Applications of Plasmonics: Nanoscopy





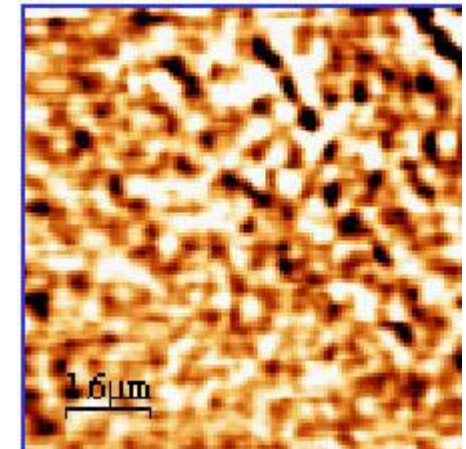
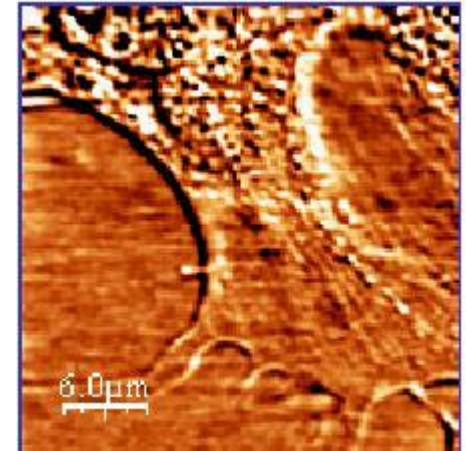
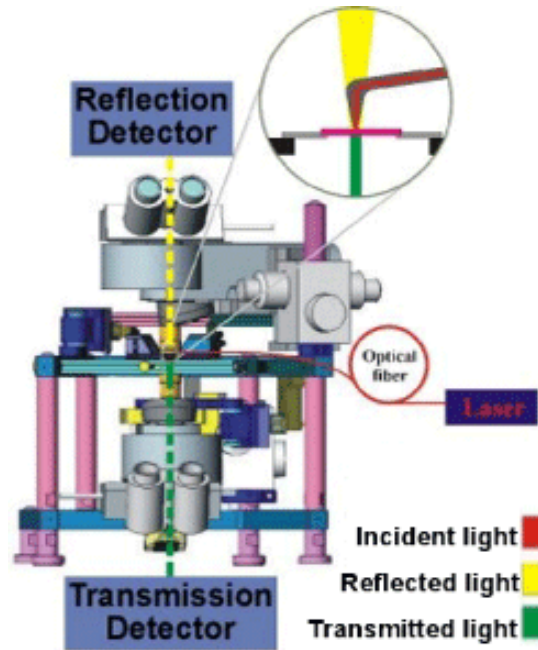
# Metal Nanosphere as an Optical Antenna in Scanning Near-Field Optical Microscope (SNOM)

P. Bharadwaj, B. Deutsch, and L. Novotny, *Optical Antennas*, *Advances in Optics and Photonics* **1**, 438–483 (2009)





NSOM images of healthy human dermal fibroblasts in liquid obtained in transmission mode with a Nanonics cantilevered tip with a gold nanosphere



L. Novotny and S. J. Stranick, *Near-Field Optical Microscopy and Spectroscopy with Pointed Probes*, Annual Rev. Phys. Chem. **57**, 303-331 (2006)

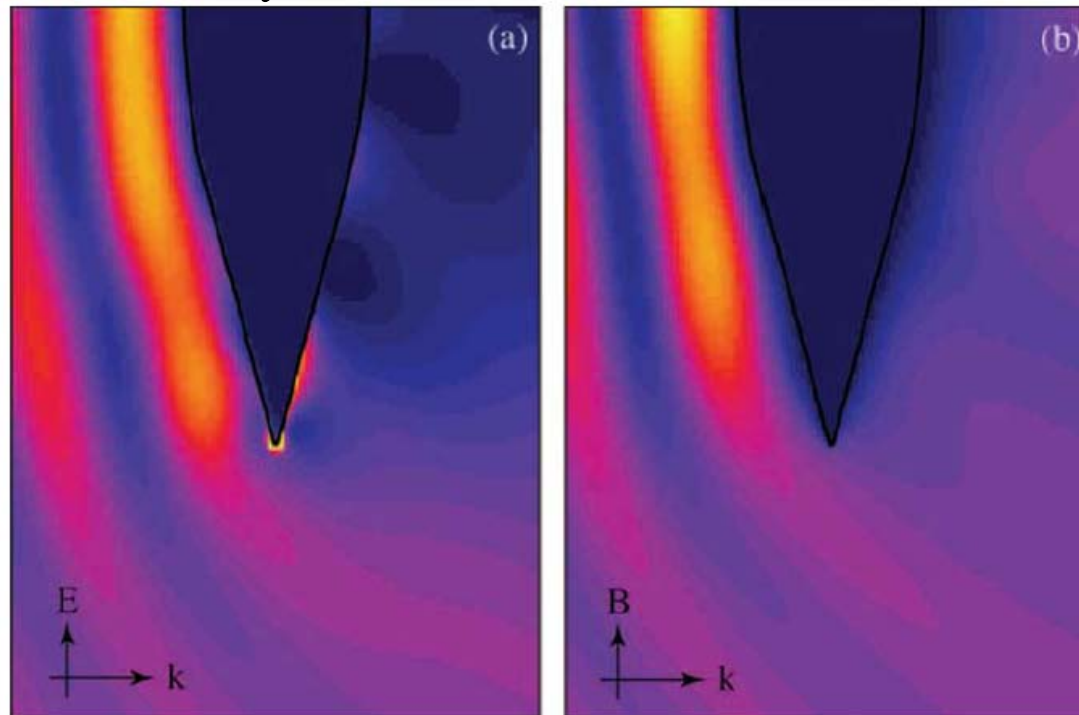


**Figure 6** Calculated intensity distribution near a laser-irradiated gold tip. The exciting wave is incident from the left and forms a standing wave pattern as it interferes with the reflected field from the tip shaft, and at the end of the tip, the wave diffracts. Two different excitation polarizations are used. The field-enhancement effect is observed only if the incident wave is polarized along the tip axis (a). In the case of an incident wave polarized perpendicular to the tip axis, the field near the tip is attenuated (b).

# Neil Anderson, Achim Hartschuh, and Lukas Novotny, *Chirality Changes in Carbon Nanotubes Studied with Near-Field Raman Spectroscopy* Nano Lett. 577 – 582 (2007)

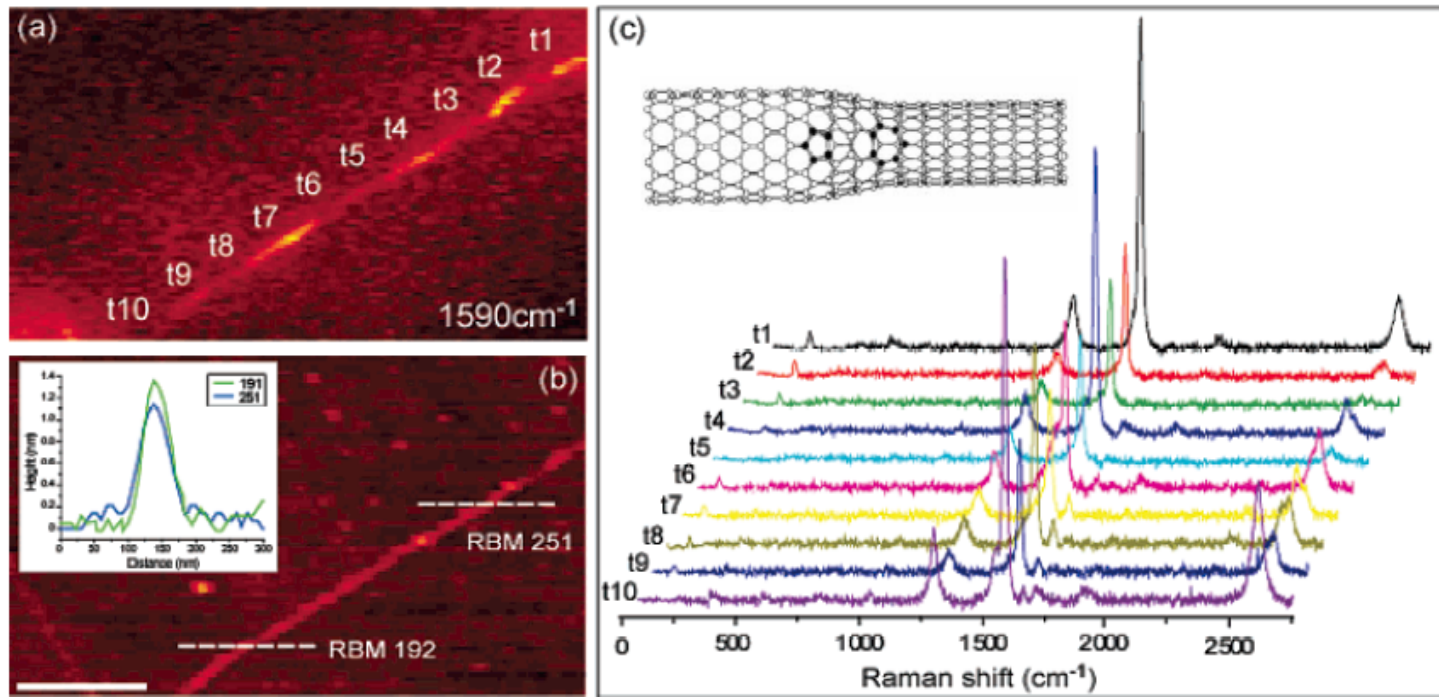


**Figure 1.** Near-field Raman imaging and spectroscopy: near-field Raman image (a) and corresponding topography image (b) of an isolated SWNT, where the optical resolution was determined to be 40 nm (fwhm). Also shown are a series of tip-enhanced Raman spectra (c) acquired along the length of the SWNT. From the recorded spectra, two resonant RBM phonons are detected. One RBM phonon frequency is detected at  $251\text{ cm}^{-1}$ , from which we assign a semiconducting chirality. The second RBM phonon frequency recorded from the lower section of the SWNT is centered at  $192\text{ cm}^{-1}$ , from which we assign a metallic chirality. See main text for details. The inset of (b) displays two cross-sectional profiles acquired from both the upper and lower sections, respectively, revealing that the expected diameter change occurs as the SWNT undergoes the transition from a semiconducting to metallic chirality. Scale bar denotes 200 nm and is valid for both (a) and (b).



T. H. Taminiau, F. B. Segerink, R. J. Moerland, L. Kuipers, and N. F. van Hulst, *Near-Field Driving of an Optical Monopole Antenna*, *Journal of Optics a-Pure and Applied Optics* **9**, S315-S321 (2007).

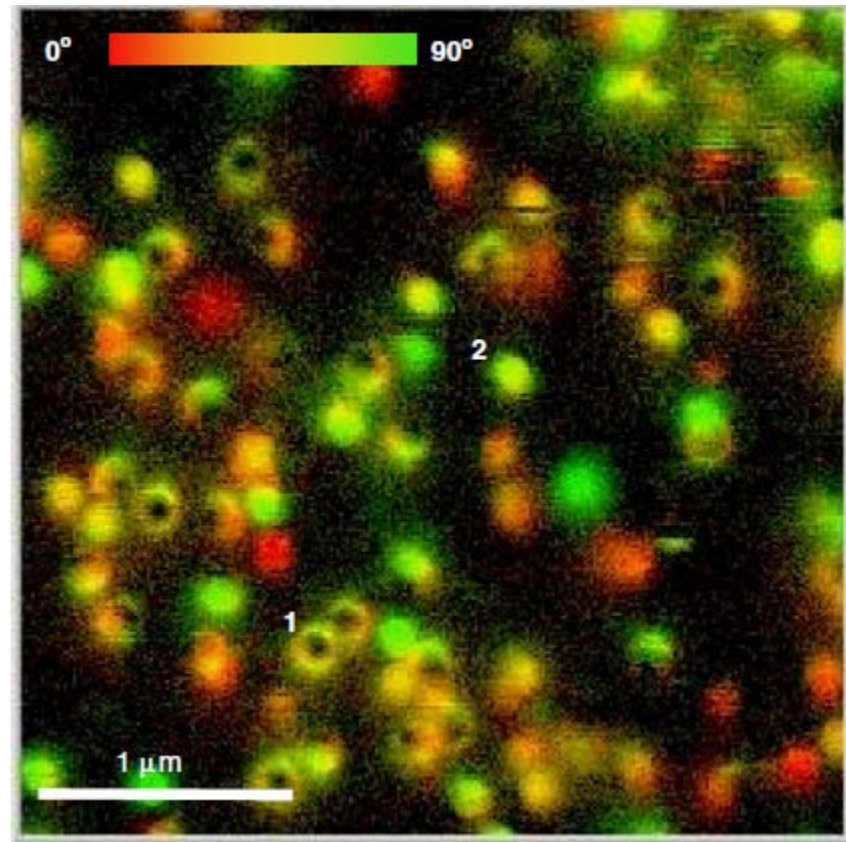
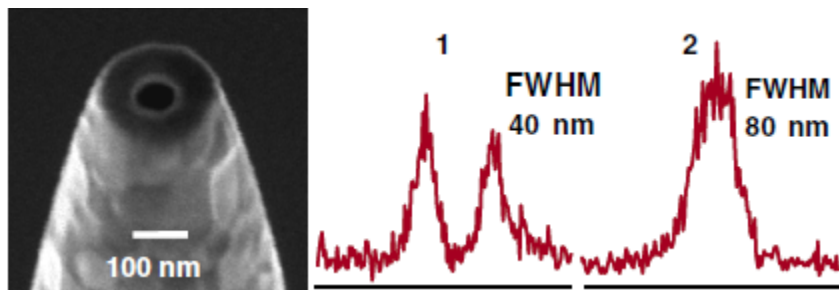
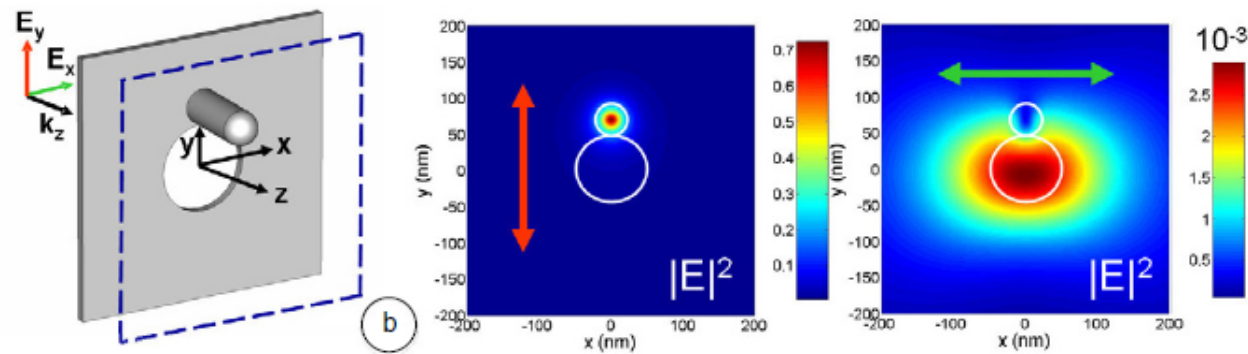
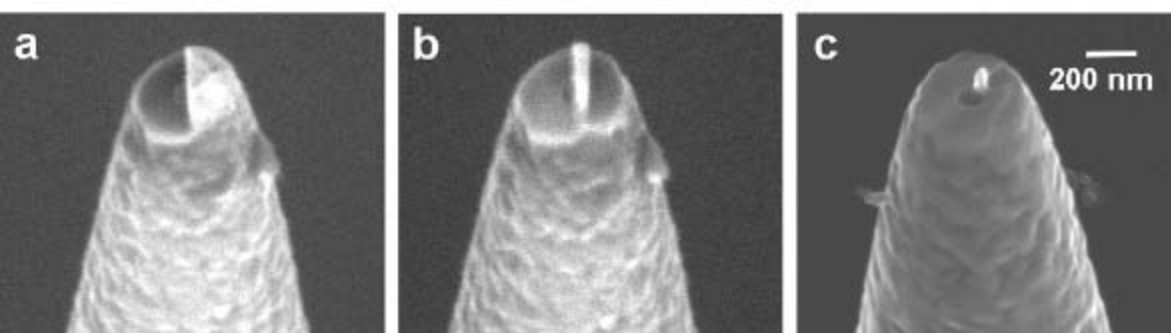
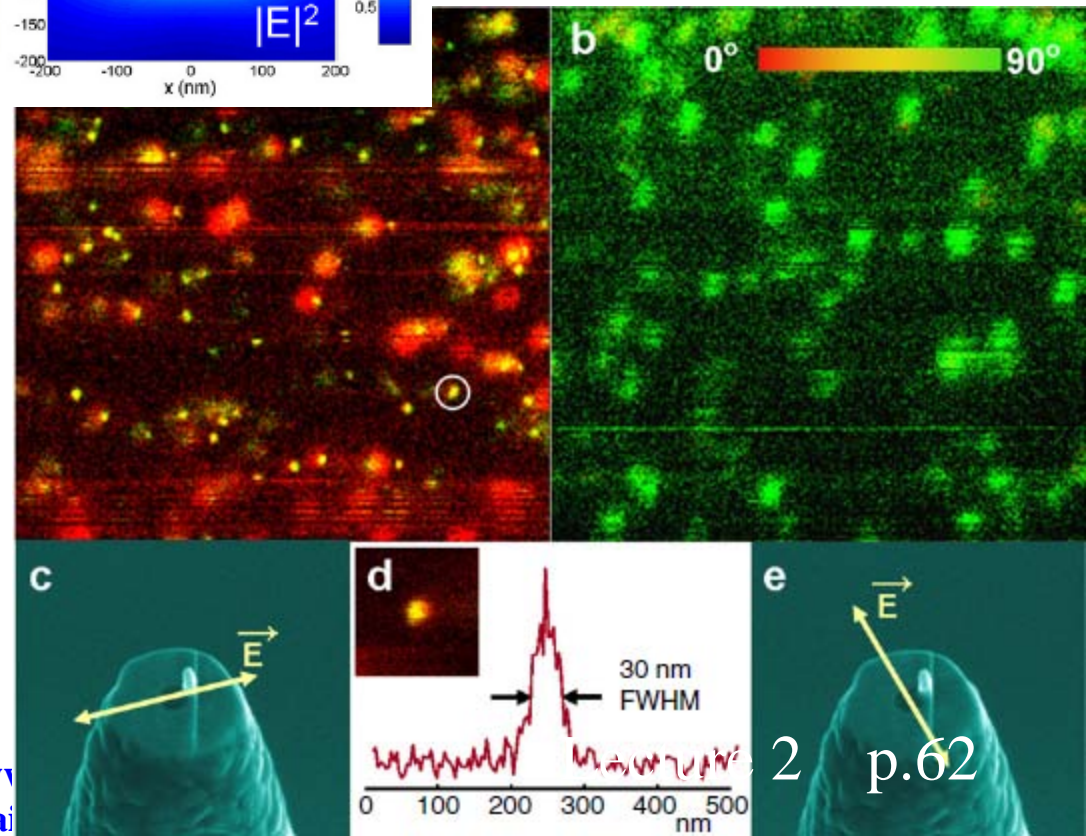


**Figure 2.** Near-field image showing the spatial fluorescence profile of several single molecules (DiI in PMMA) excited by an aperture probe. The signal is colour-coded according to the polarization of the fluorescence (red horizontal, green vertical). The inset shows a 75 nm aperture probe fabricated by FIB milling and typical fluorescence line traces for selected molecules oriented out of plane (1) and in plane (2).



Single fluorescent DiI molecules excited by the antenna probe, for two directions of incident linear polarization. Two features appear: sharp spots ( $\sim 30$  nm) showing molecules excited by the local monopole antenna and large spots ( $\sim 150$  nm) associated with molecules excited by the aperture. The sharp spots only occur in (a) for the polarization that drives the antenna. ((c), (e)) Excitation polarization with respect to the position of the antenna. (d) Fluorescence line trace for a selected molecule excited by the monopole, demonstrating the localized antenna field with 30 nm FWHM at the position of the molecule.





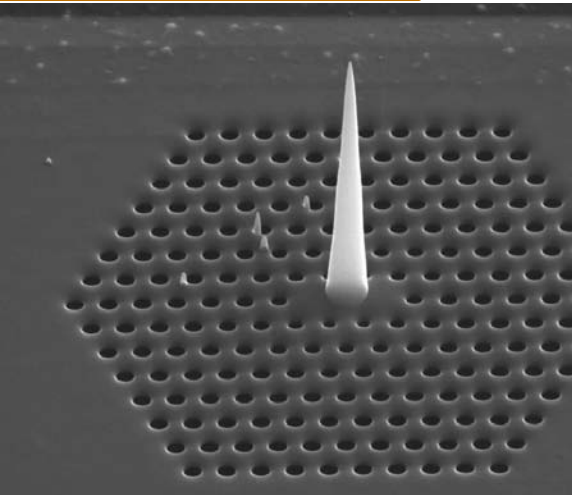
Next generation of scanning  
near-field optical microscopy  
(SNOM) with chemical  
mapping:

Adiabatic concentration of  
optical energy and giant  
surface-enhanced Raman  
scattering (SERS)

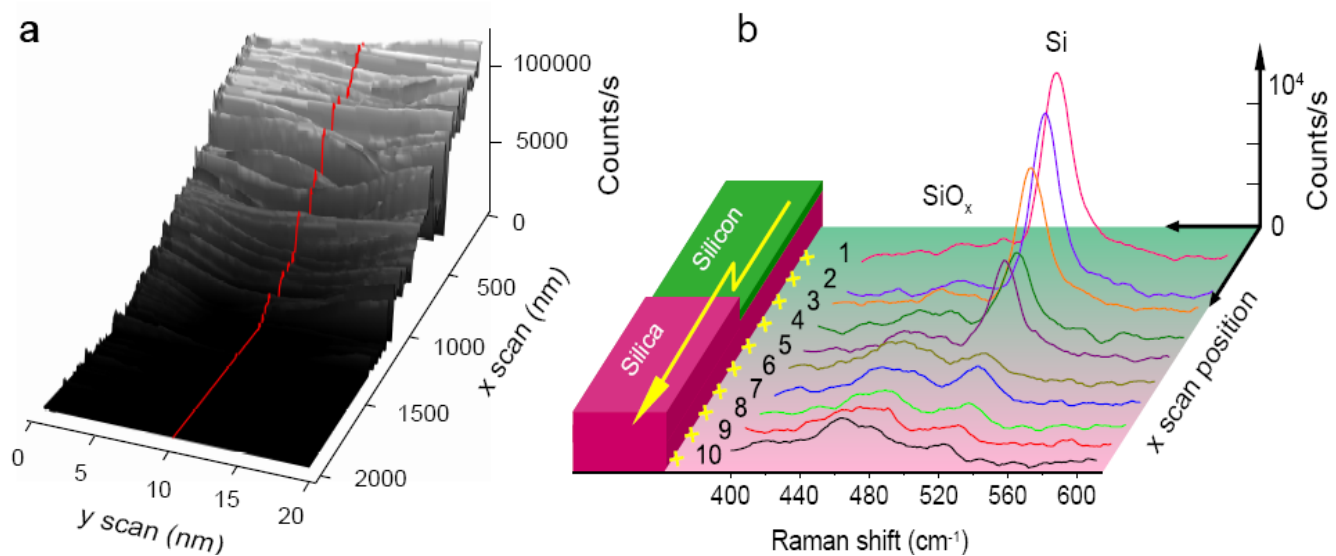


Di Fabrizio, E., *et. al*, Italian patent n. TO2008A000693 23.09.2008

5 nm radius



2/12/2008	HV	mag	WD	HPW
1:21:29 PM	30.00 kV	49999 x	5.4 mm	5.12 μm



nature nanotechnology

ARTICLES

PUBLISHED ONLINE: 22 NOVEMBER 2009 | DOI: 10.1038/NANO.2009.348

# Nanoscale chemical mapping using three-dimensional adiabatic compression of surface plasmon polaritons

Francesco De Angelis<sup>1,2</sup>, Gobind Das<sup>1</sup>, Patrizio Candeloro<sup>2</sup>, Maddalena Patrini<sup>3</sup>, Matteo Galli<sup>3</sup>, Alpan Bek<sup>4</sup>, Marco Lazzarino<sup>4,5</sup>, Ivan Maksymov<sup>3</sup>, Carlo Liberale<sup>2</sup>, Lucio Claudio Andreani<sup>3</sup> and Enzo Di Fabrizio<sup>1,2\*</sup>



# Probing the Magnetic Field of Light at Optical Frequencies

M. Burrese,<sup>1\*</sup> D. van Oosten,<sup>1</sup> T. Kampfrath,<sup>1</sup> H. Schoenmaker,<sup>1</sup>  
R. Heideman,<sup>2</sup> A. Leinse,<sup>2</sup> L. Kuipers<sup>1</sup>

*Science* **326**, 550 (2009);  
DOI: 10.1126/science.1177096

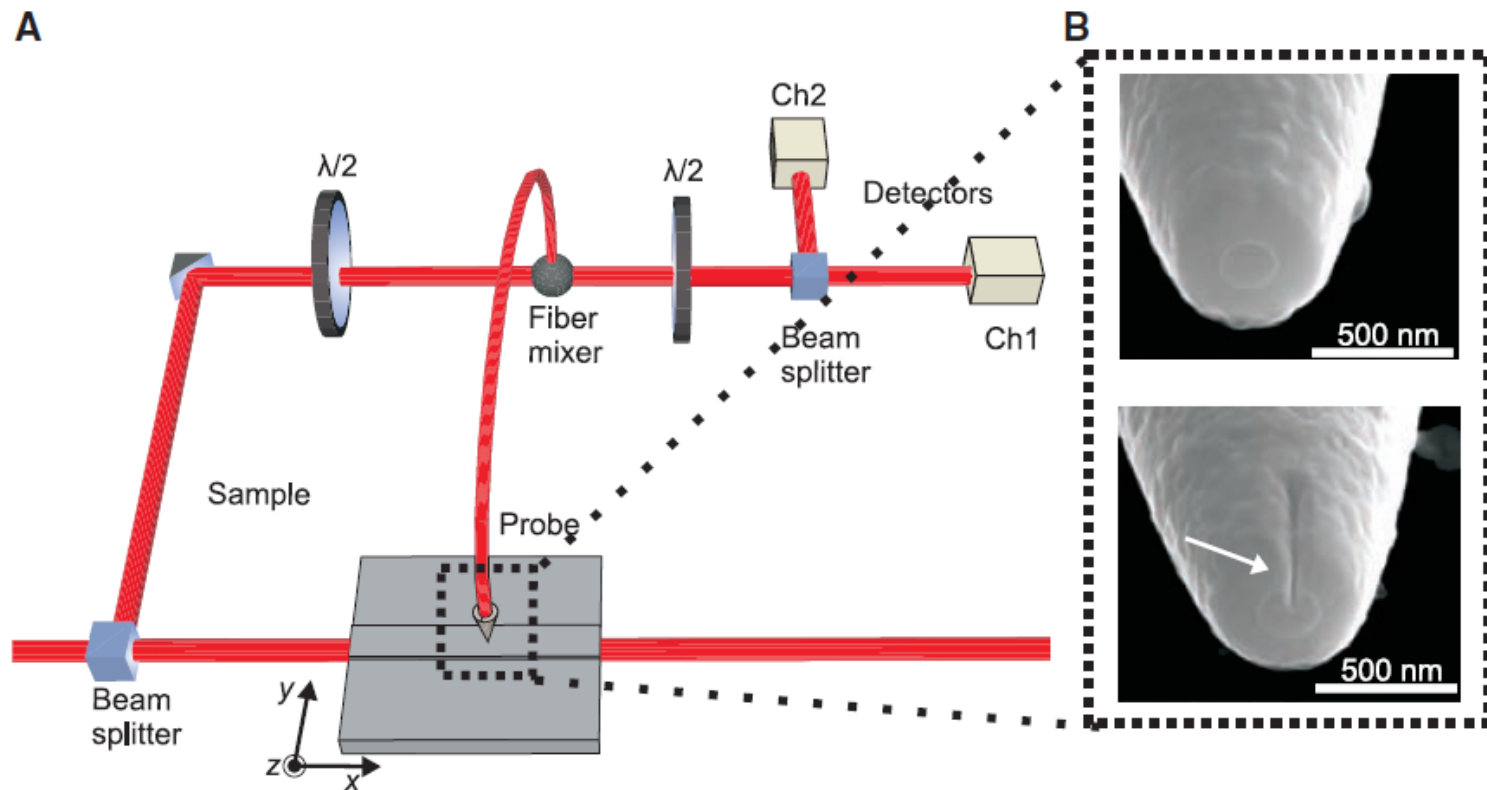
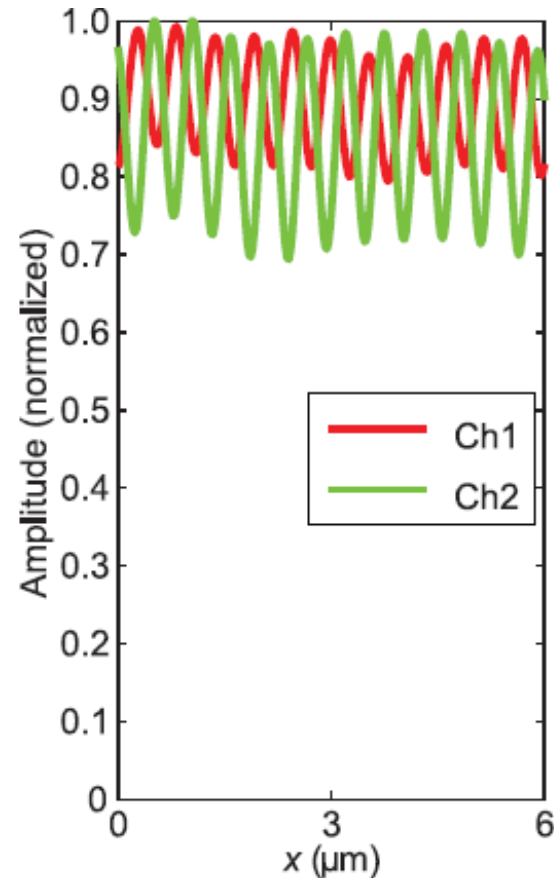
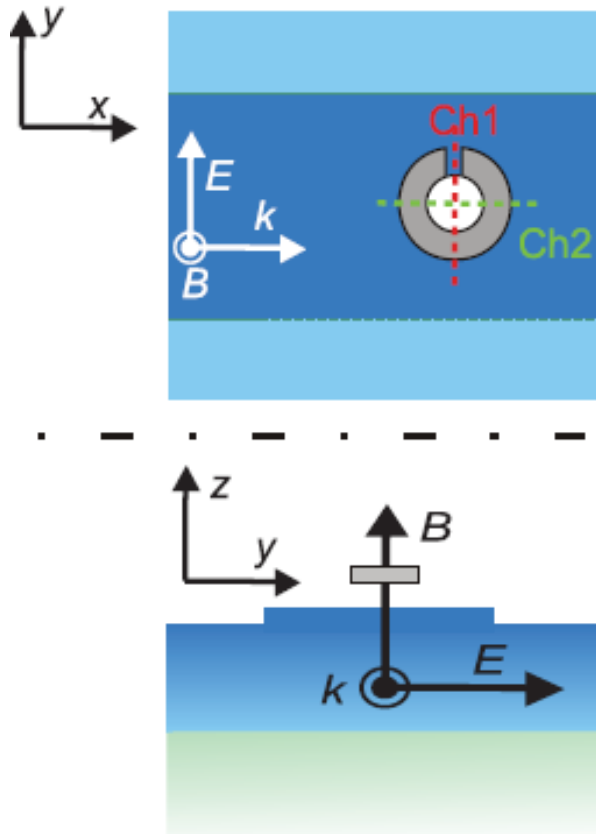


**Fig. 1.** (A) Schematic of the phase-sensitive near-field microscope. The near-field probe, indicated by the dashed box, is scanned 20 nm above the sample and collects the evanescent field of the light inside the waveguide. The light is mixed with light from a reference branch. The resulting

M. Burrese, D. van Oosten, T. Kampfrath, H. Schoenmaker, R. Heideman, A. Leinse, and L. Kuipers, *Probing the Magnetic Field of Light at Optical Frequencies*, *Science* **326**, 550-553 (2009).

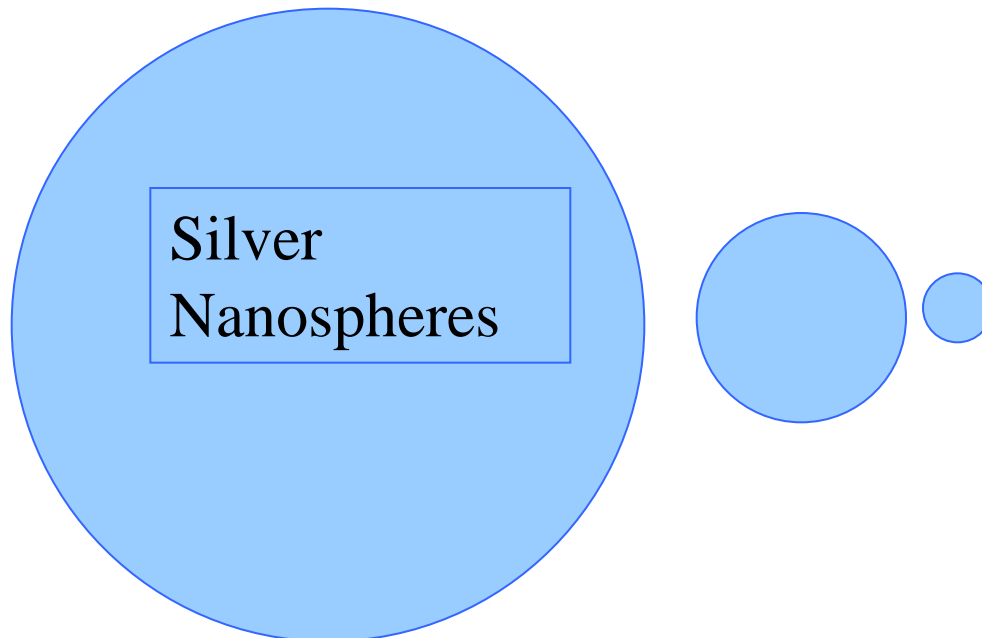


## CONCLUSIONS: Nanoscopy

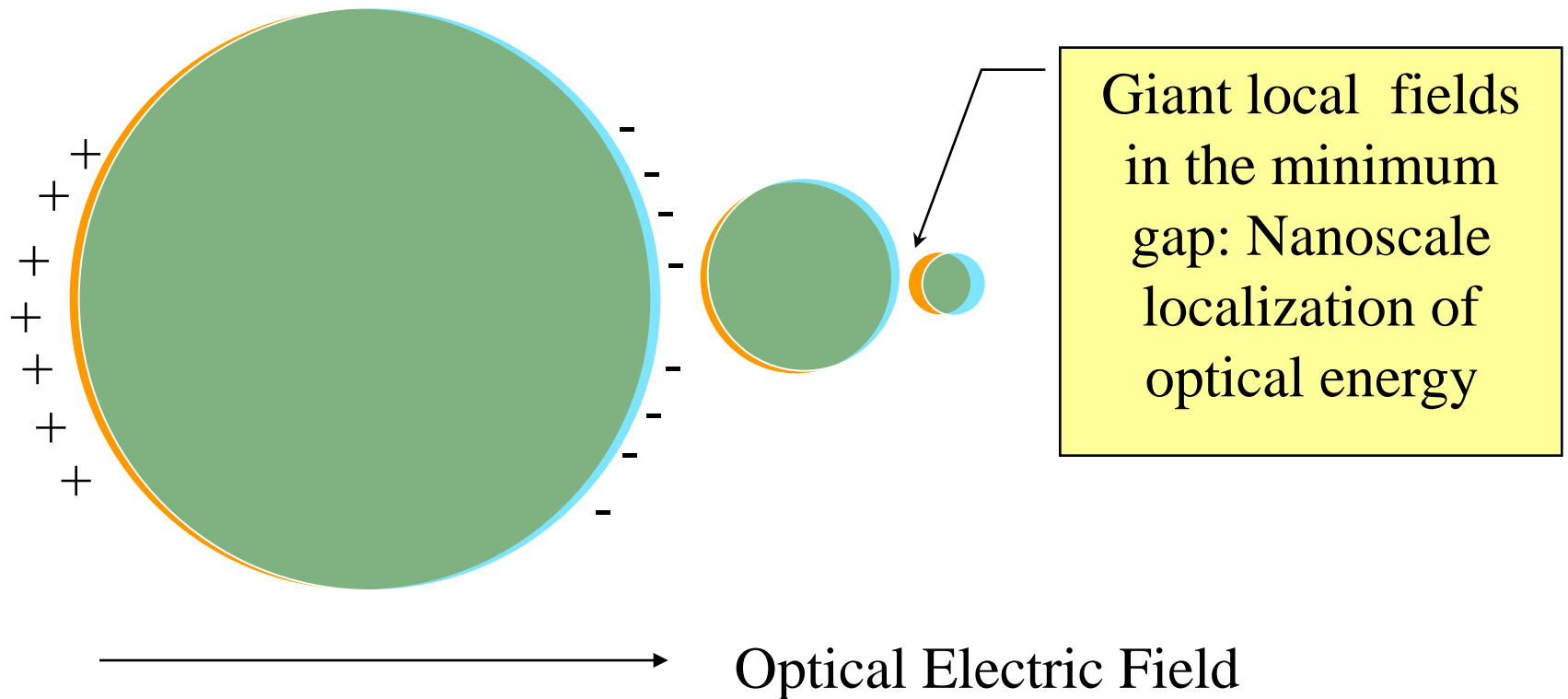
- Nanoscopy is performed with near-field probes generating nanolocalized hot spots
- There are different near-field probes: nanoparticles, pointed probes (tips) with external excitation, nanophotonic-nanoplasmonic tapered fibers, and adiabatic nanoplasmonic tapers
- The most efficient probe is an adiabatic nanoplasmonic taper that allows for SERS nanoscopy with resolution  $\sim 5$  nm
- There is a possibility to record polarization, phase, and electrical and magnetic components of the nanolocalized fields

## Efficient Self-Similar Nanolens of Nanospheres

K. Li, M. I. Stockman, and D. J. Bergman, *Self-Similar Chain of Metal Nanospheres as an Efficient Nanolens*, Phys. Rev. Lett. **91**, 227402 (2003).

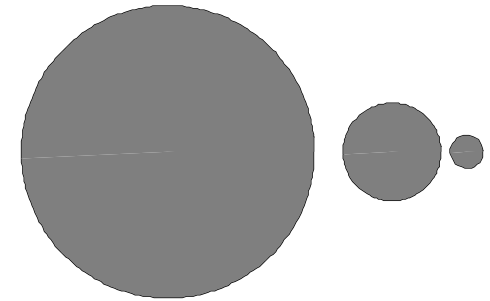


# Underlying physics of local field enhancement in efficient nanolens: Cascade enhancement



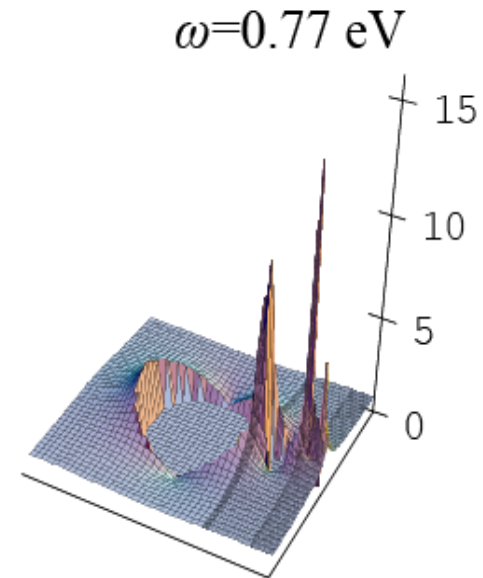
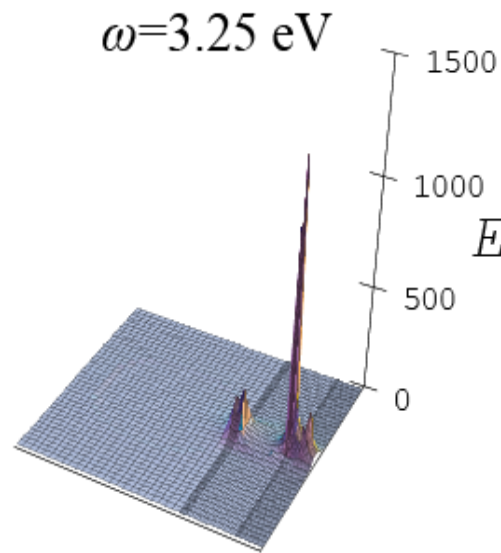
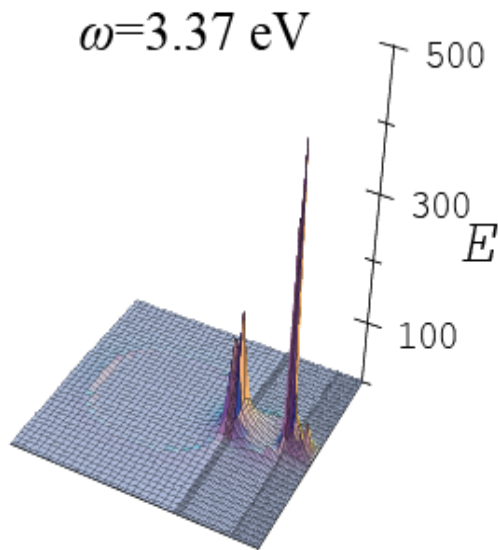
$$d=0.3R$$

## Local Fields for Silver 3-Sphere Nanolens



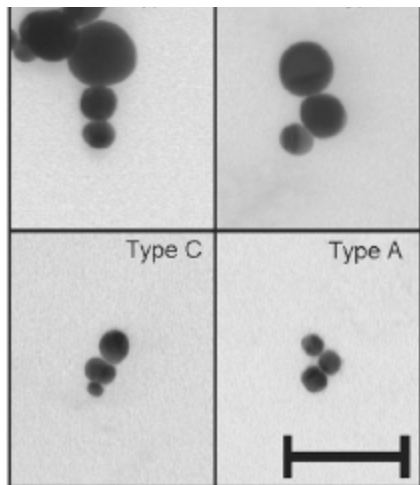
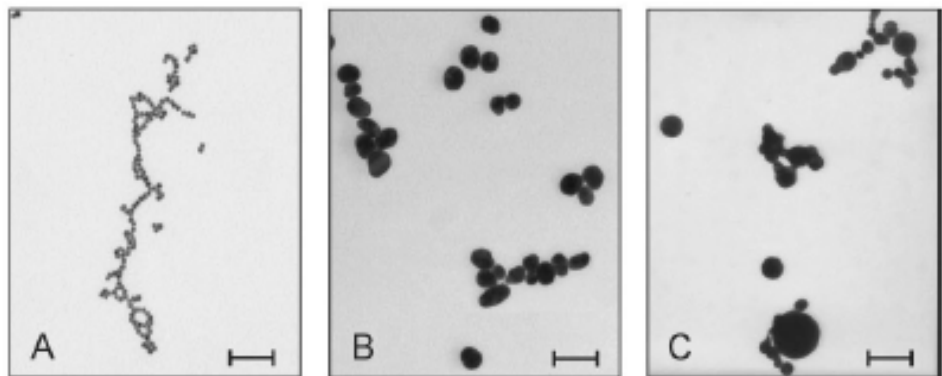
K. Li, M. I. Stockman, and D. J. Bergman, *Self-Similar Chain of Metal Nanospheres as an Efficient Nanolens*, Phys. Rev. Lett. **91**, 227402 (2003).

Raman enhancement  $\sim E^4 \sim 10^{13}$

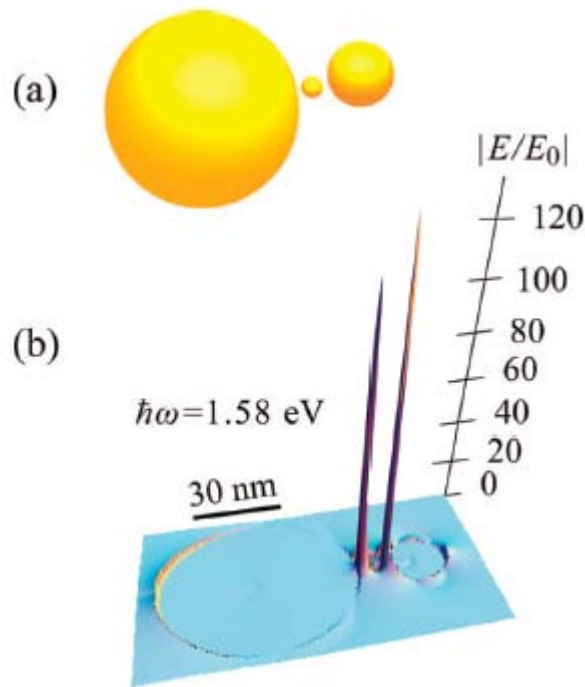


# Gold Nanolenses Generated by Laser Ablation-Efficient Enhancing Structure for Surface Enhanced Raman Scattering Analytics and Sensing

Janina Kneipp,<sup>\*,†,‡</sup> Xiangting Li,<sup>§</sup> Margaret Sherwood,<sup>†</sup> Ulrich Panne,<sup>‡</sup> Harald Kneipp,<sup>†</sup> Mark I. Stockman,<sup>§</sup> and Katrin Kneipp<sup>†,||</sup>



ics





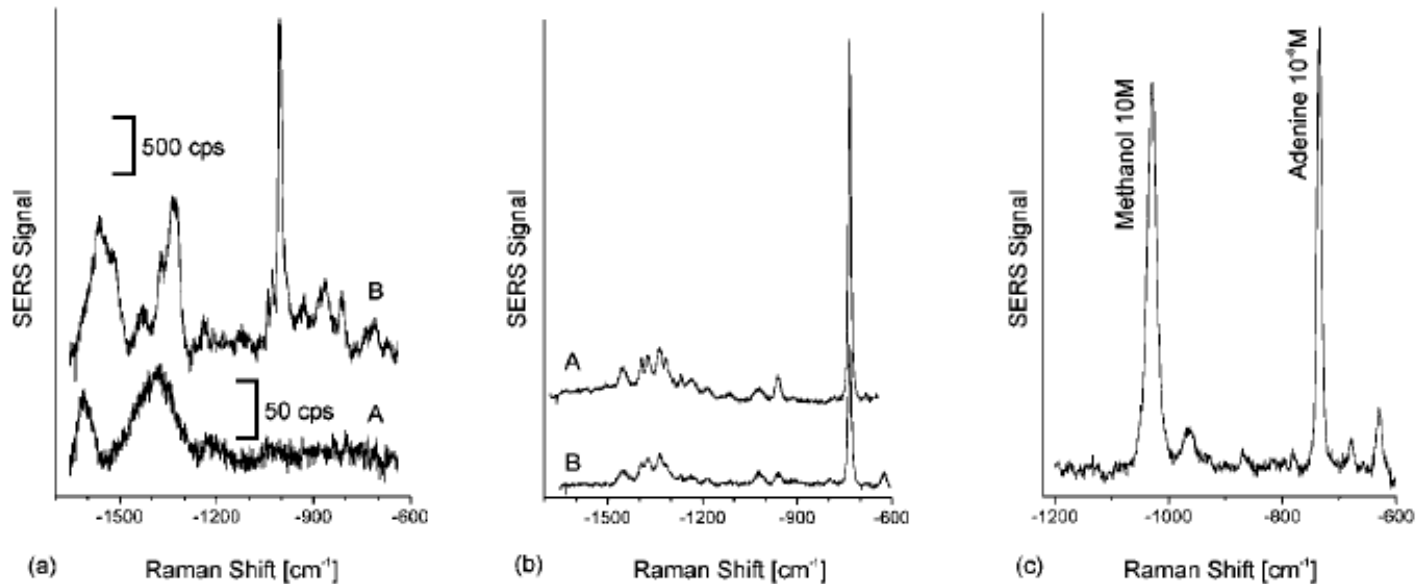


**Figure 3.** Comparison of SERS using gold nanolenses made by ablation and chemically prepared nanoaggregates as enhancing nanostructures. (a) Raman spectra measured from aqueous solutions of gold nanoaggregates without any analyte to compare background signals. The chemically prepared gold nanoparticles (spectrum B) display surface enhanced Raman lines, resulting from impurities introduced during the preparation process of this particular batch of colloids, such as the line at  $\sim 1000$   $\text{cm}^{-1}$ . The bands around  $1500$   $\text{cm}^{-1}$  in the spectrum of the ablation nanoaggregates can be assigned to carbonate complexes.<sup>18</sup> Spectra were measured at  $50$  mW at  $785$  nm excitation in  $10$  s (spectrum A) and  $1$  s (spectrum B) collection times. Abbreviation: cps, counts per second. (b) SERS signals of adenine measured in solutions of ablation aggregates (spectrum A) and chemically prepared nanoaggregates (spectrum B) using  $10$  mW at  $785$  nm excitation. (c) Comparison of the Raman signal of  $10^{-8}$  M adenine and  $10$  M methanol measured in aqueous solutions of nanoaggregates.



## Self-Similar Gold-Nanoparticle Antennas for a Cascaded Enhancement of the Optical Field

Christiane Höppener,<sup>1,2</sup> Zachary J. Lapin,<sup>1</sup> Palash Bharadwaj,<sup>1</sup> and Lukas Novotny<sup>1,\*</sup>

<sup>1</sup>*Institute of Optics, University of Rochester, Rochester, New York 14627, USA*

<sup>2</sup>*Institute of Physics, University of Münster, 48149 Münster, Germany*

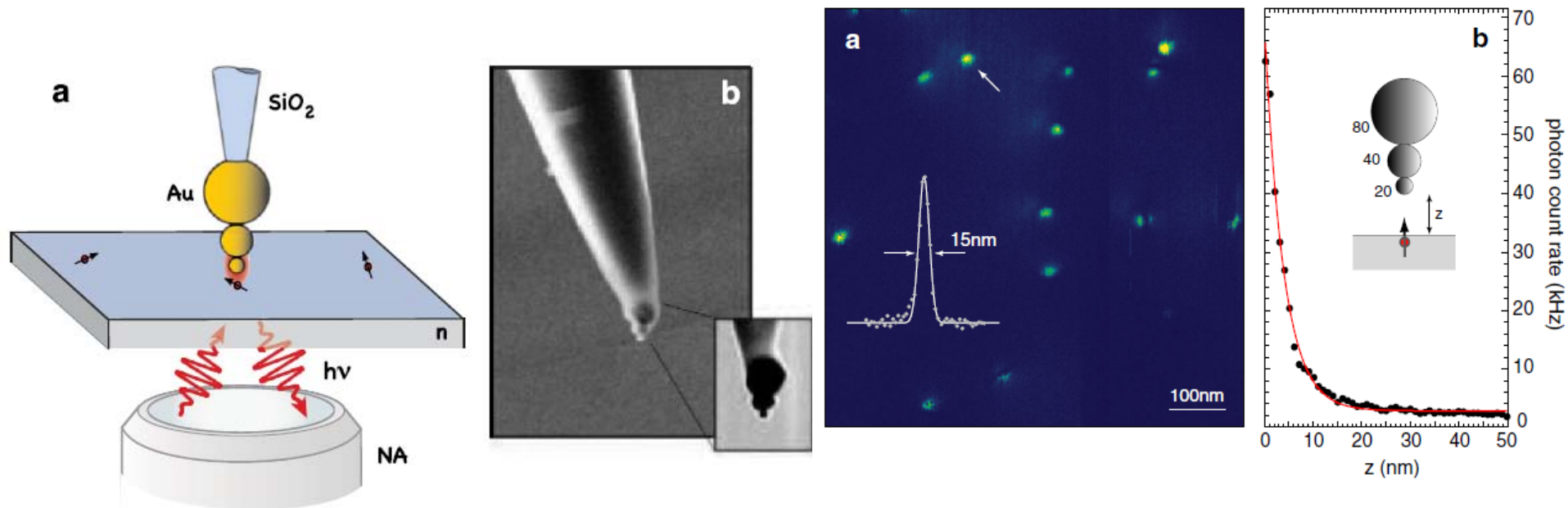


FIG. 4 (color online). Excitation of single-molecule fluorescence with a trimer antenna consisting of 80, 40, and 20 nm gold nanoparticles. (a) Fluorescence image of the single-molecule sample. Inset: Line cut through the single fluorescence spot marked by the arrow. (b) Fluorescence from a single  $z$ -oriented molecule recorded as a function of distance from a trimer antenna. The step rise of fluorescence counts for separations smaller than 15 nm is due to strong field localization along the  $z$  axis at the apex of the trimer antenna.

## CONCLUSIONS

- A self-similar chain of metal nanospheres makes an efficient nanolens focusing energy of optical field, concentrating it a nanoscale gap between the smallest nanospheres
- The optical field in the nanofocus is enhanced by more than three orders of magnitude
- A molecule adsorbed in this nanofocus will exhibit Raman scattering enhanced by a factor on order or greater than  $10^{13}$
- Using the nanolens at a tip of a SNOM renders unprecedented field concentration and spatial resolution

A dramatic sunset scene over a large body of water. The sky is filled with dark, heavy clouds, with a bright orange and red glow from the setting sun breaking through. In the foreground, the dark silhouettes of buildings are visible, including a prominent structure on the right. The water is dark, and numerous small sailboats are scattered across the horizon. The overall mood is serene and atmospheric.

END LECTURE 2